Agricultural Water Management 255 (2021) 107038

Contents lists available at ScienceDirect

Agricultural Water Management

journal homepage: www.elsevier.com/locate/agwat

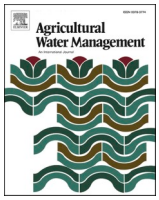

Crop water requirements and crop coefficients for jute mallow (*Corchorus olitorius* L.) using the SIMDualKc model and assessing irrigation strategies for the Syrian Akkar region

Hanaa Darouich [a,*], Razan Karfoul [b], Tiago B. Ramos [c], Ali Moustafa [b], Baraa Shaheen [b], Luis S. Pereira [a]

[a] LEAF – Landscape, Environment, Agricultural and Food, Institute of Agronomy, University of Lisbon, Tapada da Ajuda, 1349-017 Lisbon, Portugal
[b] General Commission for Scientific Agriculture Research (GCSAR), Hejaz Station, Damascus, Syria
[c] Centro de Ciência e Tecnologia do Ambiente e do Mar (MARETEC-LARSyS), Instituto Superior Técnico, University of Lisbon, Av. Rovisco Pais, 1, 1049-001 Lisbon, Portugal

ARTICLE INFO

Handling Editor-Rodney Thompson

Keywords:
Crop transpiration
SIMDualKc, Soil evaporation
Soil water balance
Water productivity

ABSTRACT

Jute mallow (*Corchorus olitorius* L.) is an annual crop grown for human consumption of its nutritious leaves in many regions of the world. Despite its importance for household food security and farmers' income, reliable information on the crop's water requirements is still quite scarce. To overcome this knowledge gap, the irrigation needs of jute mallow grown in the Akkar region in Syria were investigated. The analysis focused on a three-year period (2017–2019) where the SIMDualKc model was calibrated and validated for simulating soil water contents and computing the soil water balance in jute mallow plots irrigated with basin and drip methods. The model was further used to determine the probabilities of the demand for irrigation water in scenarios considering different crop season lengths, irrigation methods, and application depths over a longer period of 23 years (1998–2020). The SIMDualKc model was able to simulate soil water contents measured in the field plots, returning root mean square error values lower than 0.001 m^3 m^{-3} and modeling efficiencies ranging from 0.358 to 0.812. The calibrated basal (non-stressed) crop coefficients (K_{cb}) were 0.15, 0.95, and 0.95 for the initial ($K_{cb\ ini}$), mid-season ($K_{cb\ mid}$), and end-season ($K_{cb\ end}$) stages, respectively. The crop was harvested twice per season, with the drip treatments presenting the highest water productivity and economic indicators. In contrast, the basin treatment resulted in substantial percolation losses, which affected yields and indicators. Although net irrigation requirements showed a large variation for the extremes of the long-term weather time series, differences between the years representing average water demand and those representing very high water demand were only found for the drip irrigation scenarios. This study contributes to improving irrigation water management of jute mallow in the Syrian Akkar region, and for the sustainability of local production systems.

1. Introduction

Corchorus is a commercially important genus of the Malvaceae family, which comprises more than fifty species with different ethnobotanical applications (Kumari et al., 2019). Jute mallow (*Corchorus olitorius* L.) is one of the most relevant species of the Corchorus genus, widely grown for fiber production or as a leafy vegetable in Africa, Asia, and parts of Latin America and the Middle East (Choudhary et al., 2013; Kumari et al., 2019). The plant is an erect annual herb, 2–4 m tall, with lanceolate to palmate leaves, which are a rich source of carbohydrates, polysaccharides, vitamins B2, B9, C and E, minerals such as iron and calcium, β-carotene, and several phenolic compounds (Lin et al., 2009; Fondio and Grubben, 2011). The leaves are further used for medicinal purposes due to their diuretic, analgesic, antimicrobial, and antipyretic characteristics, as well as their antitumor and phenolic antioxidative constituents (Zakaria et al., 2006; Yakoub et al., 2018; Kumari et al., 2019). Lastly, the crop is cheap to produce, representing a quality food source for large segments of the population in urban and rural areas (Choudhary et al., 2013; Ngomuo et al., 2017).

In Syria, jute mallow is mainly produced as a leafy vegetable crop in

* Corresponding author.
E-mail address: hdarouich@isa.ulisboa.pt (H. Darouich).

https://doi.org/10.1016/j.agwat.2021.107038
Received 1 February 2021; Received in revised form 9 June 2021; Accepted 13 June 2021
Available online 1 July 2021

the governorates of Hama (in the Al-Ghab depression), Tartus, and Latakia, where climate conditions, the land organization in smallholdings, and the proximity of highly dense urban areas that provide for market opportunities favor the production of profitable vegetable crops (Chard, 1981; Wattenbach, 2006). In these regions, the cultivated area sums close to 1.4 M ha representing 10.2% of the Syrian cultivated land, of which 82% are irrigated (Wattenbach, 2006; CBS, 2019). The most prominent and profitable vegetables grown there are tomato (*Solanum lycopersicum* L.), cucumber (*Cucumis sativus* L.), squash (*Cucurbita pepo* L.), and eggplant (*Solanum melongena* L.), but the area cultivated with these crops including jute mallow is uncertain due to the characteristics of local production systems, which often include double cropping systems or crops cultivated in the interrow of less dense and young tree orchards.

Several policy measures were implemented in those regions as well as in other agricultural areas in Syria to rationalize agricultural water use (Oweis et al., 2003; Varela-Ortega and Sagardoy, 2003; Sadiddin, 2013; Mourad and Alshihabi, 2016; Abou Zakhem et al., 2019), improve water and economic irrigation systems productivity/performance and farmers income (Fader et al., 2016; Darouich et al., 2012, 2014, 2017), modernize irrigation methods and management (Yigezu et al., 2013; Darouich et al., 2020), and improve fertigation techniques (Janat, 2007). As a result, and despite most endeavors have been destroyed by the on-going war, modern irrigation systems have been slowly replacing traditional surface irrigation systems due to water saving policies aimed at improving land and water productivity, as well as protecting local groundwater and downstream water bodies from diffuse pollution. Therefore, drip irrigation presently supplies 43% of the irrigated area in Tartus and Latakia but only 4% in Hama (CBS, 2019), where nonetheless trends for adopting drip irrigation already exist.

Improving irrigation water use while minimizing the associated environmental risks can only be achieved through the accurate estimate of crop water requirements and appropriate irrigation schedules (irrigation timing, duration, and quantity) for maximizing yields, farmers' income, and agricultural water productivity (Pereira et al., 2002). Although jute mallow shows a remarkable value for household food security, medicinal applications, and farmers' income in many regions of the world, there is still insufficient information on the crop water needs, crop coefficients (K_c), and crop sensitiveness to water stress as shown by the knowledge gap in the recent update of tabulated FAO56 crop coefficients provided by Pereira et al. (2021) for vegetable crops.

Allen et al. (2011a, 2011b) revised a variety of field measurement approaches and related requirements for obtaining accurate estimates of evapotranspiration (ET) and crop water requirements at the field/plot scale, with appropriate focus on the combined monitoring of changes in soil water contents with the use of soil water balance models. Pereira et al. (2020a) also provided a review of soil water balance modeling approaches to determine crop ET, crop irrigation requirements, and irrigation schedules following the FAO56 method (Allen et al., 1998). This widely used method refers either to the single K_c or to the dual K_c approach to determine crop evapotranspiration as the product of a crop coefficient and the grass reference evapotranspiration (ET_o). The latter is computed with the FAO Penman-Monteith (FAO-PM) equation and crop evapotranspiration may be measured by several methods as described and discussed by Allen et al. (2011a) and Pereira et al. (2020a). Unfortunately, existing papers on crop coefficients for jute mallow use reference ET different from the standard ET_o, which may make their use highly biased. Therefore, there is the need to derive accurate K_c from field ET_c data and the FAO-PM ET_o.

The dual K_c approach, which partitions crop evapotranspiration (ET_c) into its components crop transpiration (T_c) and soil evaporation (E_s), also partitions K_c into the basal crop coefficient (K_{cb}) referring to T_c, and the soil evaporation coefficient (K_e). This approach results more precise, namely because it improves the estimation accuracy of the evaporation component (Pereira et al., 2015a, 2020a). The dual K_c approach is widely applied for estimating evapotranspiration fluxes of crops grown under different climatic regions and management practices (López-Urrea et al., 2009; Paço et al., 2012; Kool et al., 2014; González et al., 2015; Paredes et al., 2018a, 2018b). Similarly, the SIMDualKc model (Rosa et al., 2012a), which adopts the FAO56 dual K_c approach, has been applied to various crops, including a winter wheat–summer maize crop sequence (Zhao et al., 2013), soybean (Wei et al., 2015), and tomato (Zhang et al., 2018) in the North of China; potato in southern Italy (Paredes et al., 2018a); maize in Brazil and Uruguay (Martins et al., 2013; Giménez et al., 2016), and bermudagrass in Brazil (Paredes et al., 2018b). The SIMDualKc model was further used in Syria to estimate crop coefficients and water use of wheat (Rosa et al., 2012b) and of zucchini squash under diverse irrigation regimes (Darouich et al., 2020). The reported variety of applications in terms of crops, environmental and weather conditions, as well as management practices, assures the suitability of the model for the present study.

Considering the brief review above, the objectives of this study are: (i) to simulate soil water contents in jute mallow plots irrigated with basin and drip methods using the SIMDualKc model during three growing seasons (2017–2019); (ii) to derive the crop coefficients for jute mallow grown in the Syrian Akkar plain using the dual K_c approach; (iii) to evaluate the components of the soil water balance from a water saving and economic perspective; and (iv) to define seasonal irrigation thresholds based on the crop's net irrigation requirements computed using a long-term weather time series that may serve as guidelines for defining future water saving policies. Results of this study will contribute to improving irrigation water use performance in the Syrian coastal region where the Akkar plain is located, and for the sustainability of jute mallow production in the region.

2. Material and methods

2.1. Field experiment

2.1.1. Description of the study site

The field experiment was performed at the Zahid research center (34°41'37''N, 35°59'16''E, 12 m a.s.l.), in the western part of the Akkar plain, Tartus governorate, Syria, from May 2017 to August 2019. The Akkar Plain is located on a narrow coastal area of fertile land between the cities of Tartus, in Syria, and Trípoli, in Lebanon. The region is especially suited to produce field and greenhouse-grown vegetables due to favorable environmental and climate conditions, the proximity of highly dense urban areas, and water resources availability (Wattenbach, 2006).

The climate in the region is classified as Hot-summer Mediterranean climate (Csa; Köppen, 1884). The mean annual air temperature is 19.3 °C, while the mean daily temperatures range from a minimum of 11.5 °C in January to a maximum of 27.0 °C in August. The mean annual precipitation is 930 mm, which occur mostly between October and May. The mean annual reference evapotranspiration (ET_o) computed with the FAO56 Penman-Monteith equation (Allen et al., 1998) is 1363 mm for the period 1998–2020. The dominant soil reference groups are Vertisols, Cambisols, and Luvisols (FAO/IIASA/ISRIC/ISS-CAS/JRC, 2009). Surface water resources include the Al-Abrash, Al-Janoubi, Kalife, Abo Falat, and Ostouene rivers, which supply 29,100 ha of irrigated agricultural land in Tartus and 38,000 ha in Latakia, complemented with groundwater resources (CBS, 2019). The depth of these groundwater resources varies between 10 and 20 m (Abou Zakhem and Hafez, 2007).

2.1.2. Experimental design and treatments

The experimental design used to study the soil water balance of zucchini squash in the same region (Darouich et al., 2020) was also adopted for jute mallow, known locally as *molokhia*. The experiment involved irrigation with basin and drip methods and various schedules during the 2017, 2018, and 2019 growing seasons. The experimental area, with 23 m long and 19 m wide (437 m^2), was flat, with 0.005% and 0.002% slope in the west and south directions, respectively. The soil was

classified as a Vertisol (IUSS Working Group WRB, 2014), with the main soil physical and chemical properties given in Table 1. Disturbed and undisturbed soil samples were collected for the layers 0–0.15, 0.15–0.30, 0.30–0.45, and 0.45–0.60 m, by opening a small trench in the area adjacent to the experiment. The particle size distribution (%) was measured with a hydrometer following the USDA texture classification limits (Soil Survey Staff, 2011). The dry bulk density (ρ_b) was obtained by drying volumetric soil samples (100 cm^3) at 105ºC for 48 h. The organic matter (OM) content, which quantifies the organic fraction of the soil on a mass basis, was estimated from the OC (organic carbon) content determined by the Walkley–Black method, using the relation OM = 1.724 × OC (Nelson and Sommers, 1982). The soil water content at saturation (θ_S; $m^3\ m^{-3}$) was determined from the maximum volumetric water content of 100 cm^3 undisturbed soil cores. The soil water contents at field capacity (θ_{FC}; $m^3\ m^{-3}$) and the wilting point (θ_{WP}; $m^3\ m^{-3}$) were measured on undisturbed soil samples of 100 cm^3 using the pressure plate apparatus (Dane and Hopmans, 2002).

The experimental plots were organized in a randomized complete block design, with three treatments (T0, T1, T2), and four replicates per treatment (Fig. 1). Each replicate was 9 m long and 2 m wide (18 m^2), with 7 sowed rows spaced 0.30 m apart. Seeds were sowed at a depth of 0.5–1.5 cm and irrigated with 10–20 mm of applied water to aid germination. Replicates distanced 1 m from each other.

Table 2 presents the sowing and harvest dates as well as the respective dates of the crop growth stages during the three growing seasons. Two harvests were obtained per season. Irrigation was performed from sowing to harvest. The water was conveyed from a well to the field by a PVC mainline and distributed to three polyethylene manifold pipes. The drainage network was buried at a depth of 1.25–1.75 m, with drainpipes distancing 15–25 m. Treatment T0 represented the traditional irrigation scheme followed by farmers in the region. In this treatment, plants were irrigated by basin irrigation, with water supplied by one of the manifold pipes, which discharged approximately 15 $m^3\ h^{-1}$. Irrigation was applied with an elapsed time of 0.60–0.70 h until the basin was completely flooded. Table 3 presents the basin irrigation amounts, with irrigation events succeeding on average every 10 days depending on weather conditions. Treatments T1 and T2 refer to drip irrigation schemes. Laterals were disposed along each plant row. In-line drippers were spaced 0.2 m, with a discharge rate of 4 L h^{-1} at 100 kPa. Both treatments aimed to fulfill crop water requirements and maximize water productivity. However, irrigation was triggered considering different thresholds. Irrigation in T1 and T2 was initiated when soil water contents in the rootzone dropped respectively below 90% and 80% of the soil water content at field capacity (θ_{FC}). Irrigation events succeeded on average every 5–6 days in T1 and 6–10 days in T2 depending on the season. Irrigation depths (Table 3) were estimated in the field based on atmospheric demand and soil moisture measurements following a simple water balance procedure. Soil water contents were measured at depths of 0.2 and 0.4 m, every week, by gravimetry. Three soil samples were randomly collected per depth and treatment.

Additional management practices included fertilization with manure (30 Mg ha^{-1}), phosphorus (125 kg ha^{-1}), and potassium (65 kg ha^{-1}) before sowing. Nitrogen was applied as urea (57.5 kg N ha^{-1}) in two batches, one 3–4 weeks after sowing and the other after the first harvest. Weed control was performed manually.

2.2. Modeling approach

2.2.1. Model description

The SIMDualKc model (Rosa et al., 2012a) uses a daily time step to compute the soil water balance at the plot scale as follows:

$$D_{r,i} = D_{r,i-1} - (P - RO)_i - I_i - CR_i + ET_{c\ act,i} + DP_i \quad (1)$$

where D_r is the root zone depletion (mm), P is the rainfall (mm), RO is the surface runoff (mm), I is the net irrigation depth (mm), CR is the capillary rise from the groundwater table (mm), $ET_{c\ act}$ is the actual crop evapotranspiration (mm), and DP is the deep percolation from the root zone (mm), all referring to day i or day i-1.

The model adopts the FAO56 dual K_c approach for computing crop evapotranspiration (Allen et al., 1998, 2005; Rosa et al., 2012a). In this approach, the components relative to crop transpiration (T_c, mm) and soil evaporation (E_s, mm) are estimated separately as:

$$T_c = K_{cb}\ ET_o \quad (2)$$

$$E_s = K_e\ ET_o \quad (3)$$

where K_{cb} is the standard basal crop coefficient (-), K_e is the evaporation coefficient (-), and ET_o is the grass reference evapotranspiration (mm) computed using the FAO56 Penman–Monteith equation (Allen et al., 1998). $ET_{c\ act}$ is obtained as a function of the available soil water in the root zone by introducing a dimensionless stress coefficient (K_s), which affects the T_c component:

$$ET_{c\ act} = T_{c\ act} + E_s \quad (4)$$

$$T_{c\ act} = K_{cb\ act}\ ET_o = K_s\ K_{cb}\ ET_o \quad (5)$$

where $T_{c\ act}$ is the actual crop transpiration (mm), and $K_{cb\ act}$ is the actual basal crop coefficient (-). K_s, which values vary from 0 to 1, is defined as:

$$K_s = \frac{TAW - D_{r,i}}{TAW - RAW} \quad (6)$$

in which TAW and RAW are respectively the total and readily available soil water relative to the rooting depth (mm). These are computed as:

$$TAW = 1000\ Z_r\ (\theta_{FC} - \theta_{WP}) \quad (7)$$

$$RAW = p\ TAW \quad (8)$$

where θ_{FC} and θ_{WP} are the soil water contents at field capacity and the wilting point ($m^3\ m^{-3}$), respectively, Z_r is the root depth (m), and p is the depletion fraction for no stress (-). When soil depletion exceeds the depletion fraction for no stress, i.e., the soil water content drops below RAW, T_c values are reduced due to water stress ($K_s < 1.0$); otherwise, no reduction in T_c values occurs ($K_s = 1.0$).

For a crop with two cuts like jute mallow, the K_{cb} curves are described for each cutting cycle considering four growth stages: (i) the initial stage or start of the crop season; (ii) the rapid growth or development stage; (iii) the mid-season stage, which corresponds to the

Table 1
Main soil physical and chemical properties in the experimental area.

Depth (m)	Soil texture (%)			ρ_b (g cm^{-3})	OM (%)	Water content			TAW (mm)
	Sand (2.0–0.05 mm)	**Silt (0.05–0.002 mm)**	**Clay (<0.002 mm)**			**θ_S ($m^3\ m^{-3}$)**	**θ_{FC} ($m^3\ m^{-3}$)**	**θ_{WP} ($m^3\ m^{-3}$)**	
0.0–0.15	15	28	57	1.24	2.15	0.532	0.512	0.230	42.3
0.15–0.30	16	32	52	1.25	1.95	0.528	0.473	0.242	34.7
0.30–0.45	20	30	50	1.30	1.91	0.509	0.476	0.242	35.1
0.45–0.60	19	28	53	1.43	–	0.531	0.514	0.298	32.4

ρ_b, bulk density; OM, organic matter content; θ_S, soil water content at saturation; θ_{FC}, soil water content at field capacity; θ_{WP}, soil water content at the wilting point; TAW, total available water.

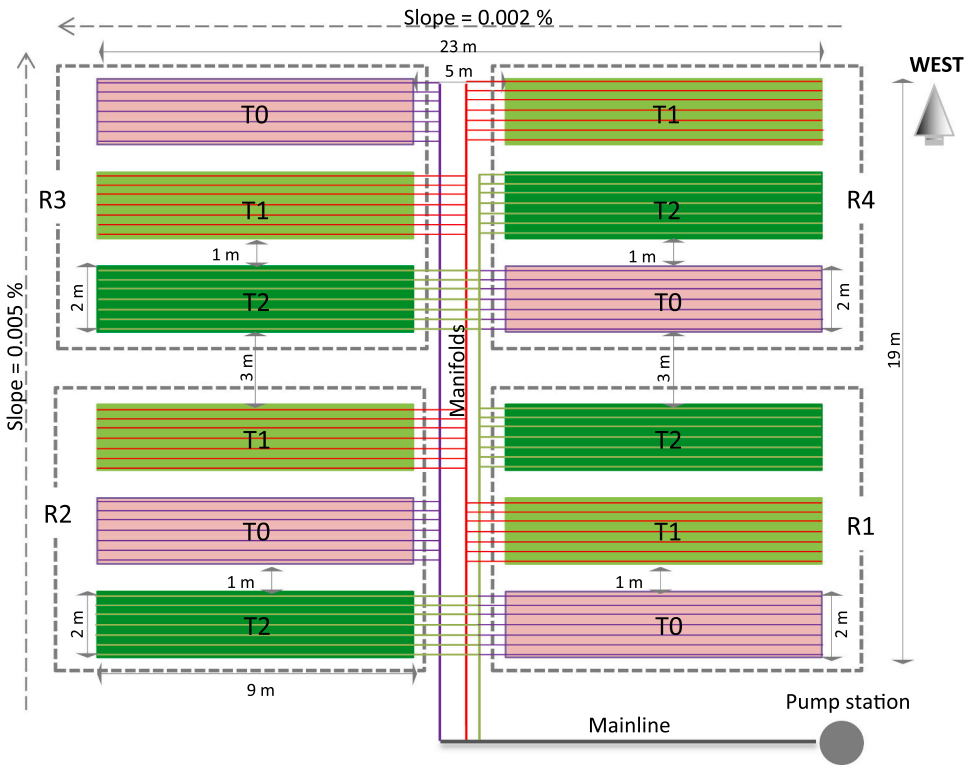

Fig. 1. Schematic layout of the experimental area.

Table 2
Dates and length (number of days) of the crop growth stages.

Year	Cut		Crop growth stages					Total (days)
			Initial	**Rapid growth**	**Mid-season**	**Late season**	**Harvest**	
2017	1st	Dates	May 28	June 03	June 20	July 17	July 17	–
		Lengths	6	17	27	1	–	51
	2nd	Dates	July 18	July 22	August 04	August 31	August 31	–
		Lengths	4	13	27	1	–	45
2018	1st	Dates	May 16	May 23	June 02	June 30	June 30	–
		Lengths	7	10	28	1	–	46
	2nd	Dates	July 01	July 02	July 08	July 22	July 22	–
		Lengths	1	6	14	1	–	22
2019	1st	Dates	May 01	May 11	May 26	June 22	June 22	–
		Lengths	10	15	27	1	–	53
	2nd	Dates	June 23	June 25	July 03	July 21	July 21	–
		Lengths	2	8	18	1	–	29

Table 3
Irrigation treatments.

Year	T0 Basin irrigation			T1 Drip irrigation			T2 Drip irrigation		
	N° events	**Depth per event (mm)**	**Total (mm)**	**N° events**	**Depth per event (mm)**	**Total (mm)**	**N° events**	**Depth per event (mm)**	**Total (mm)**
2017	9	110	990	17	11–30	421	10	13–43	393
2018	5	110	550	11	11–24	219	10	10–35	200
2019	7	115	805	18	11–23	308	13	11–32	291

T0, T1, T2, experimental treatments.

period when plant's canopy is maximum; and (iv) the late-season stage. Curves are described by three K_{cb} values corresponding to the initial, mid- and end-season stages, respectively $K_{cb\ ini}$, $K_{cb\ mid}$, and $K_{cb\ end}$. These values were calibrated based on field observations of soil water contents taking into consideration the recommendations for accuracy by Allen et al. (2011a). $K_{cb\ mid}$ and $K_{cb\ end}$ are further internally corrected to local climatic conditions when the average RH_{min} differs from 45%, and the average u_2 differs from 2 m s^{-1} (Allen et al., 1998; Pereira et al., 2021) as follows:

$$K_{cb} = K_{cb\ calib} - [0.04\ (u_2 - 2) - 0.004\ (RH_{min} - 45)]\left(\frac{h}{3}\right)^{0.3} \quad (9)$$

where K_{cb} corresponds to the K_{cb} standard values and $K_{cb\ calib}$ are the K_{cb} values obtained from calibration. The K_{cb} values may be further adjusted to actual crop characteristics (density and height) using a density coefficient (K_d), which accounts for the increase in K_{cb} with the increase in the amount of vegetation (Allen and Pereira, 2009; Pereira et al.,

2020b).

Soil evaporation is limited by the amount of energy available at the soil surface in conjunction with the energy consumed by transpiration, and by water availability in the surface soil layer (Allen et al., 1998, 2005). E_s is maximum during the early crop stages when crop shadowing is small and the topsoil is wetted by rain or irrigation and energy is largely available at the soil surface. On the other hand, E_s is minimum when the crop fully shadows the soil, limiting the energy available for evaporation, and/or when the surface soil layer is dry. Thus, the evaporation coefficient (K_e) is computed as follows (Allen et al., 2005):

$$K_e = K_r\,(K_{c\ max} - K_{cb\ min}) \le f_{ew}\,K_{c\ max} \quad (10)$$

where K_r is the evaporation reduction coefficient (values range from 0 to 1), $K_{c\ max}$ is the maximum value of K_c (i.e., $K_{cb} + K_e$) following a rain or irrigation event (-), and f_{ew} is the fraction of the soil that is both exposed to radiation and wetted by rain or irrigation (-), which depends upon the fraction of ground covered by the crop (f_c). K_r is obtained following the two-stage drying cycle approach where the first stage is the energy limited stage, and the second is the water limited stage (Ritchie, 1972; Allen et al., 1998, 2005):

$$K_r = 1 \text{ for } D_{e,i-1} \le REW \quad (11)$$

$$K_r = \frac{TEW - D_{e,i-1}}{TEW - REW} \text{ for } D_{e,i-1} > REW \quad (12)$$

where TEW and REW are respectively the total and readily evaporable water in the evaporation soil layer (mm), and D_e is the evaporation layer depletion at the end of day i−1 (mm). D_e is computed through a daily water balance of the evaporation soil layer, with the evaporation decreasing as the evaporable soil water decreases in the evaporation soil layer beyond REW.

Finally, deep percolation (DP) is computed using the parametric time decay function proposed by Liu et al. (2006), which relates the soil water storage above field capacity with the draining time until θ_{FC} is reached:

$$W_a = a_D\,t^{b_D} \quad (13)$$

where W_a is the actual soil water storage in the root zone (mm), a_D is the soil water storage comprised between saturation (θ_s) and θ_{FC} (mm), b_D is an empirical dimensionless parameter, and t is the time after an irrigation or rain that produces storage above field capacity (days). Runoff (RO) is estimated using the curve number approach (USDA-SCS, 1972).

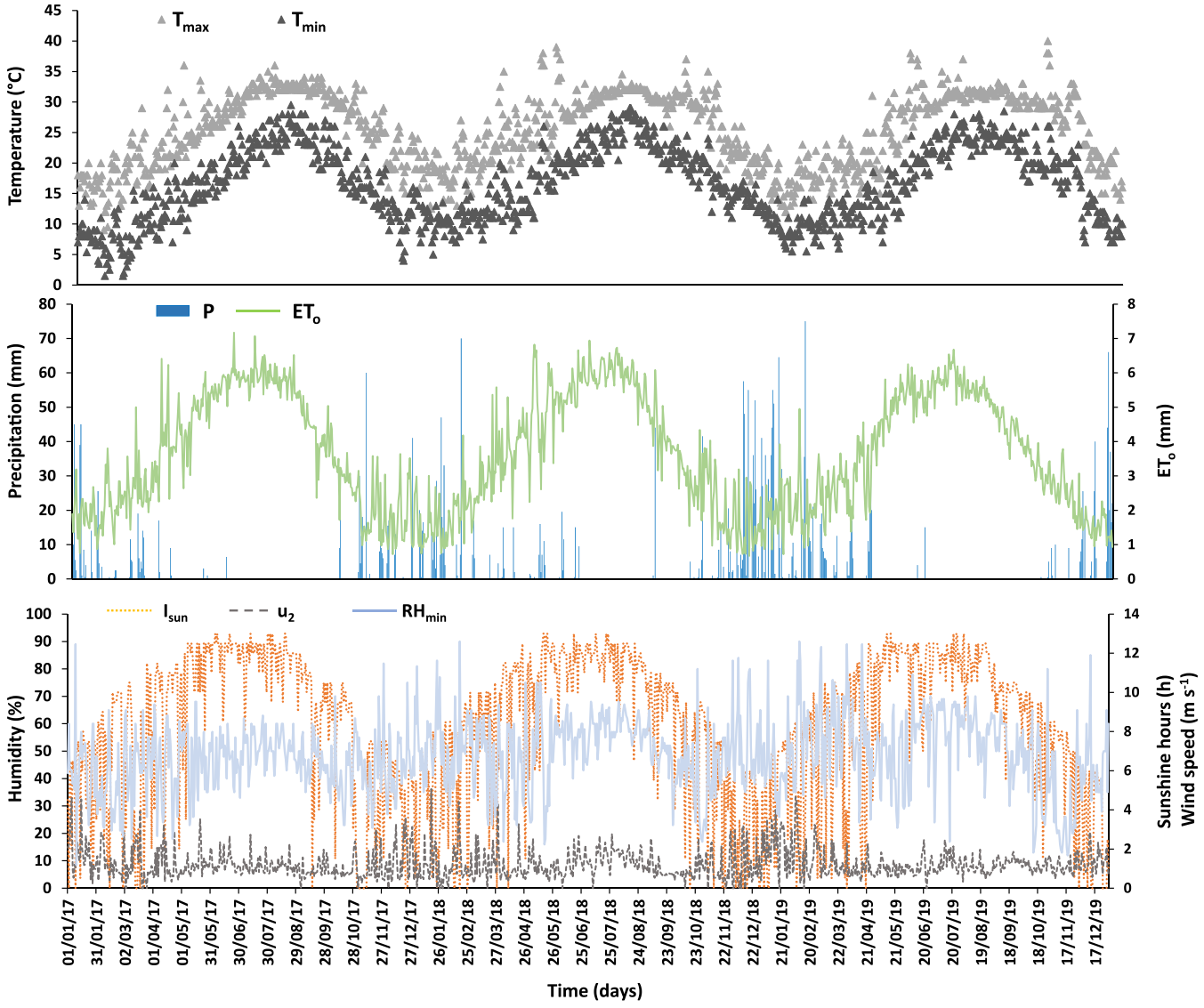

Fig. 2. Daily maximum (T_{max}, °C) and minimum (T_{min}, °C) air temperatures, minimum relative humidity (RH_{min}, %), number of sunshine hours (I_{sun}, h), wind speed (u_2, m s^{-1}), precipitation (mm), and grass reference evapotranspiration (ET_o, mm) for the 2017–2019 years.

Capillary rise (CR) was not considered in this study due to the existence of a drainage network in the study area.

2.2.2. Model setup

The SIMDualKc model requires detailed information on weather conditions, soil properties, crop phenology, irrigation events, and irrigation systems to compute the soil water balance. Meteorological conditions were observed at the local weather station placed over a well-watered clipped grass during the three experimental seasons and are displayed in Fig. 2. The available information included daily values of maximum and minimum surface air temperatures (T_{min} and T_{max}, °C), minimum and maximum relative humidity (RH_{min}, RH_{max}, %), sunshine hours (I_{sun}, h), wind speed measured at 2 m height (u_2, m s^{-1}), and rainfall (P, mm).

The soil profile was characterized using the particle size distribution and soil hydraulic properties of the different soil layers listed in Table 1. The TAW (mm) values were then obtained automatically from θ_{FC}, θ_{WP}, and layer thickness. The depth of the evaporation layer (Z_e) was specified according to Allen et al. (1998, 2005), and the values of TEW and REW were calculated according to the soil texture and water holding characteristics of the soil evaporation layer. The curve number (CN) was also specified based on the particle size distribution of the surface soil layer as well as land use (USDA-SCS, 1972). The deep percolation parameters relative to the parametric equation of Liu et al. (2006) were defined according to the soil texture data, and θ_s and θ_{FC} values in the soil profile. Lastly, the initial soil water depletion values in both the root zone and the evaporation soil layer were defined based on measurements taken in the different treatments at the beginning of each growing season, resulting 25–35% of TAW and 25–35% of TEW, which correspond to expected low soil wetness conditions by early May.

Crop phenology data included the observed dates of the initial, rapid growth, mid-season, and late-season stages as well as the harvest dates of each growing season (Table 2), which refer to end-season. The $K_{cb\ ini}$, $K_{cb\ mid}$, and $K_{cb\ end}$ were then specified based on Pereira et al. (2021) values for leaves vegetable crops. The soil water depletion fraction values for no stress (p_{ini}, p_{mid}, p_{end}) were also set for the same crop stages following Pereira et al. (2021). Crop height (h), the estimated fraction of ground cover (f_c), and root depth (Z_r) were defined for each crop stage based on observations and are presented in Table 4. Crop height (h) and the mean canopy width were monitored using a tape at each stage, and mainly before and after each harvest. The fraction of ground cover (f_c) was then estimated based on the surface area between rows covered by the canopy (assuming a rectangular shape of the canopy). Root depth (Z_r) was observed in soil profiles at the end of each crop season. Leaves were collected in all replicates after each harvest and the fresh weight was recorded.

Finally, referring to irrigation data, the dates of irrigation events and irrigation depths were specified according to observations. The fraction of the soil surface wetted by irrigation (f_w) was further measured and defined as 0.3 in the drip treatments and 1.0 in the basin irrigation treatment.

2.2.3. Model calibration and validation

The SIMDualKc model was calibrated following an "iterative trial and error" procedure, which consisted of adjusting model parameters one at a time within reasonable ranges of values until deviations between measured and simulated soil water contents were minimized. The 2018 dataset from the three treatments was selected for calibration. Calibration, following Pereira et al. (2015b), started by first adjusting the $K_{cb\ ini}$, $K_{cb\ mid}$, and $K_{cb\ end}$, and the corresponding p_{ini}, p_{mid}, and p_{end} parameters; then, the deep percolation parameters a_D and b_D; and in a third step, the Z_e, REW, and TEW. Model calibration was considered terminated when the best fit was achieved, and the errors of prediction did not change from an iteration to the next. If that goal was not achieved at the end of the first trial and error cycle, the calibration process restarted again. Validation was then performed by comparing measured soil water contents with the respective model predictions using the previously calibrated model parameters. The 2017 and 2019 datasets were used for validation.

Table 4
Measured crop state variables.

Year	Cut	Crop growth stages			
		Initial	Rapid growth	Mid-season	Harvest
f_c (-)	**1st**	0.05	0.65	0.95	0.95
	2nd	0.50	0.80	0.95	0.95
h (m)	–	0.05	0.50	0.90–1.0	0.90–1.0
Z_r (m)	–	–	–	–	0.60

f_c, soil cover fraction; h, crop height; Z_r, root depth.

The model performance was evaluated using various goodness-of-fit indicators, including the regression coefficient (b_0), the coefficient of determination (R^2), the root mean square error (RMSE), the ratio of the RMSE to the standard deviation of observed data (NRMSE), the percent bias of estimation (PBIAS), and the modeling efficiency (NSE), respectively given as (Nash and Sutcliffe, 1970; Legates and McCabe, 1999; Moriasi et al., 2007):

$$b_0 = \frac{\sum_{i=1}^{n} O_i P_i}{\sum_{i=1}^{n} O_i^2} \tag{12}$$

$$R^2 = \left\{ \frac{\sum_{i=1}^{n} \left(O_i - \overline{O}\right)\left(P_i - \overline{P}\right)}{\left[\sum_{i=1}^{n} \left(O_i - \overline{O}\right)^2\right]^{0.5} \left[\sum_{i=1}^{n} \left(P_i - \overline{P}\right)^2\right]^{0.5}} \right\}^2 \tag{13}$$

$$RMSE = \sqrt{\frac{\sum_{i=1}^{n} (O_i - P_i)^2}{n-1}} \tag{14}$$

$$NRMSE = \frac{RMSE}{\overline{O}} \tag{15}$$

$$PBIAS = 100 \quad \frac{\sum_{i=1}^{n} (O_i - P_i)}{\sum_{i=1}^{n} O_i} \tag{16}$$

$$NSE = 1 - \frac{\sum_{i=1}^{n} (O_i - P_i)^2}{\sum_{i=1}^{n} \left(O_i - \overline{O}\right)^2} \tag{17}$$

where O_i and P_i are respectively the observed and model predicted values at time i, $\overline{O}$ and $\overline{P}$ are the respective mean values, and n is the number of observations. b_0 values close to 1 indicate that the predicted values are statistically close to the observed ones. R^2 values close to 1 indicate that the model explains well the variance of observations. RMSE and NRMSE values close to zero indicate small estimation errors and good model predictions (Legates and McCabe, 1999). PBIAS values close to zero indicate that model simulations are accurate, while positive or negative values indicate under- or over-estimation bias, respectively. NSE values close to 1 indicate that the residuals' variance is much smaller than the observed data variance, hence the model predictions are good. On the contrary, if NSE is less than zero the model-predicted values are worse than simply using the observed mean (Nash and Sutcliffe, 1970).

2.3. Water productivity indicators

The experimental results were further assessed using the crop water productivity indicators relative to the total water used (WP_{WU}, kg m^{-3}), the irrigation water applied (WP_{Irrig}, kg m^{-3}), the consumptive use (WP_{ET}, kg m^{-3}), and transpiration (WP_T, kg m^{-3}), which were described

Table 5
Jute mallow growing degree days (GDD) during the experimental period.

Year	Cut	GDD per crop stage (°C)s				Total GDD (°C)
		Initial stage	Rapid growth	Mid-season	Late-season	
2017	1st	43	165	325	11	544
	2nd	53	180	377	12	622
2018	1st	88	89	303	13	493
	2nd	32	52	183	14	281
2019	1st	51	119	272	12	454
	2nd	34	101	250	13	397
Average	1st	61	124	300	12	497
	2nd	39	111	270	13	433

in Pereira et al. (2009a, 2012, 2020a) and Fernández et al. (2020), and are respectively given by:

$$WP_{WU} = \frac{Y_a}{TWU} \quad (18)$$

$$WP_{Irrig} = \frac{Y_a}{IWU} \quad (19)$$

$$WP_{ET} = \frac{Y_a}{ET_{c\ act}} \quad (20)$$

$$WP_{T} = \frac{Y_a}{T_{c\ act}} \quad (21)$$

where Y_a is the actual (measured) yield (kg ha^{-1}), TWU is the total water used given by the sum of effective P, I, and the variation of the soil water storage (ΔSW) (m^3 ha^{-1}), IWU is the irrigation water used (m^3 ha^{-1}), $ET_{c\ act}$ is the estimated actual evapotranspiration (m^3 ha^{-1}), and $T_{c\ act}$ is again the estimated actual crop transpiration (m^3 ha^{-1}).

The economic crop water productivity (EWP, $ m^{-3}) and the economic crop water productivity ratio (EWPR) were also computed as follows (Pereira et al., 2009a, 2012; Fernández et al., 2020):

$$EWP = \frac{Value(Y_a)}{TWU} \quad (22)$$

$$EWPR = \frac{Value(Y_a)}{Cost(TWU)} \quad (23)$$

where Value(Y_a) is the value of the achieved yield ($ ha^{-1}), and Cost (TWU) is the cost of the irrigation water ($ ha^{-1}). EWP expresses the ratio between the profit produced by a crop along the growing season and the total amount of water involved in crop production. The EWPR shows the impacts of water prices on the economic return of irrigation. The yield value was here set to 0.22 $ kg^{-1} according to prices from CAPMAS (2020) in Egypt, which can also be considered representative for the Syrian market. The price of the irrigation water was set to 0.055 $ m^{-3} as in Darouich et al. (2020).

Yields and water productivity indicators in the different treatments and growing seasons were also subjected to a two-way ANOVA analysis using SPSS statistical software version 25.0 (SPSS Inc., Chicago, IL, USA). The significant level was tested for different levels of probability using Yates's weighted squares of means (Yates, 1934).

2.4. Net irrigation requirements

Net irrigation requirements (NIR) consist of the amount of water that needs to be applied to the crop to fully satisfy its water needs when the water available through precipitation, capillary rise, and soil water storage variation is insufficient (Pereira et al., 2020a). NIR of jute mallow were computed using a weather time series for the period 1998–2020 (23 years), which included all daily records of T_{max} and T_{min}, RH_{max} and RH_{min}, I_{sun}, u_2 at 2 m height, and P available in the same local meteorological station used in the experiment since its installation. Missing u_2 values in 2011–2013 and 2015 were filled with wind data from the closest weather station (Trípoli, Lebanon). For each year, simulations were performed using the calibrated crop parameters, while initial soil water depletion was set as 25% of TAW and 25% of TEW following the earlier observations from irrigation treatments. The sowing and crop stages dates were defined as follows:

A. The sowing date in each simulated year was set to May 1st, which corresponds to the common beginning of the jute mallow season in the region. The dates of the crop growth stages were then defined based on the mean cumulative growing degree days (GDD) observed during the three growing seasons (Table 5). The base temperature was 15 °C following Fondio and Grubben (2011).
B. The sowing and crop stages dates were set as in the 2017 season, which corresponded to the latest sowing date and longest growing season observed in the experiment.

On the other hand, irrigation scheduling considered the following strategies:

I. Basin irrigation with a Management Allowed Depletion (MAD) equal to the depletion fraction for no stress (p) (MAD = p), in which net irrigation depths were computed to refill soil water contents to field capacity.
II. Drip irrigation with MAD = p, in which net irrigation depths were fixed to 20 mm per event.

Table 6
Default and calibrated model parameters.

Parameters	Default values	Calibrated values
$K_{cb\ ini\ I}$	0.20	0.15
$K_{cb\ mid\ I}$	0.95	0.95
$K_{cb\ end\ I}$	0.30	0.95
$K_{cb\ ini\ II}$	0.20	0.35
$K_{cb\ mid\ II}$	0.95	0.95
$K_{cb\ end\ II}$	0.30	0.95
$p_{ini\ I}$	0.40	0.55
$p_{mid\ I}$	0.40	0.55
$p_{end\ I}$	0.40	0.55
$p_{ini\ II}$	0.40	0.55
$p_{mid\ II}$	0.40	0.55
$P_{end\ II}$	0.40	0.55
TEW (mm)	31	17
REW (mm)	8	8
Z_e (m)	0.10	0.05
a_D	–	475
b_D	-0.0173	-0.02
CN	85	85

K_{cb}, basal crop coefficient for the initial ($K_{cb\ ini}$), mid ($K_{cb\ mid}$), and end-season ($K_{cb\ end}$) stages; p, depletion fraction for no stress during the initial (p_{ini}), mid (p_{mid}), and end-season (p_{end}) stages; TEW, total evaporable water; REW, readily evaporable water; Z_e, depth of the soil evaporation layer; a_D and b_D, deep percolation parameters; CN, curve number. The subscripts I and II denote for the first and second cut cycle, respectively.

For each scenario (AI, AII, BI, BII), the probability of the demand for irrigation water for the period 1998–2020 was computed by identifying the years representing the average, high, and very high demand, which correspond respectively to the probabilities of 50%, 80% and 95% for non-exceedance as in Pereira et al. (2009b).

3. Results and discussion

3.1. Model parametrization

Table 6 presents the model parameters calibrated during the 2018 growing season, which were then validated during the 2017 and 2019 seasons. The calibrated $K_{cb\ ini\ I}$ and $K_{cb\ ini\ II}$ values were 0.15 and 0.35, respectively (subscripts I and II denote for the first and second cut cycles). The higher $K_{cb\ ini}$ value relative to the second cycle resulted from the larger f_c value (0.50) of plants remaining in the field after the first cut, with the crop already well-established when compared with the period after sowing (Table 4). For these reasons, the length of the initial stage during the second cut cycle was short (Table 2). The calibrated $K_{cb\ mid}$ value was 0.95 for both cut cycles. Lastly, the calibrated $K_{cb\ end}$ value was also set to 0.95 in both cut cycles, thus indicating that harvesting for fresh human consumption was done when jute mallow leaves were still green and tender, i.e., before senescence occurs. These options agree with those proposed by Pereira et al. (2021) for $K_{cb\ mid}$ and $K_{cb\ end}$ of leaves and flowers vegetable crops. As such, and because experimental plots were relatively small and fast to harvest, only one day was considered as the length of the late-season stage (Table 2). For larger crop areas where harvesting of leaves takes several days, it could be assumed a longer late-season and a shorter mid-season, with $K_{cb\ end}$ decreasing to 0.35 as described in Fig. 3. As a result of leaves harvesting, crop transpiration would progressively decrease, thus K_{cb} would reduce gradually from 0.95 to 0.35. This hypothesis needs, however, to be confirmed.

As referred earlier, the literature on jute mallow water requirements is quite scarce, with existing studies lacking detailed information on crop phenological characteristics and with non-precise derivation of K_c. Moreover, no studies were found where jute mallow was harvested with two cuts. Considering this information gap, the calibrated $K_{cb\ mid}$ and $K_{cb\ end}$ values matched the corresponding tabulated K_{cb} values for the mid and end-season stages of most leaves vegetable crops listed in Pereira et al. (2021).

The p_{ini}, p_{mid}, and p_{end} values were set to 0.55 during both cut cycles, representing an increase from those proposed by Allen et al. (1998) and Pereira et al. (2021) for leaves vegetable crops (Table 6). Jute mallow was thus considered to be more tolerant to water stress than those crops during the different crop stages.

3.2. Model simulation of the soil water contents

Fig. 4 presents the soil water contents measured in the root zone of treatments T0, T1, and T2 during the 2017–2019 growing seasons, and compares these values with the SIMDualKc simulations. Fig. 4 further provides the dates of rainfall and irrigation events as well as depths applied per event.

The seasonal irrigation depths in T0 ranged from 550 to 990 mm, with water applied through basin flooding in 5–9 events (Table 3). Irrigation scheduling in this treatment followed the common practice in the region, which finds some comparison with the management of jute mallow in other parts of the world (Palada and Chang, 2003; Odofin et al., 2011). While the seasonal amount of water depended much on the length of the crop's growing season, the depths applied per irrigation event were very similar and characteristically high, ranging from 110 to 115 mm. As a result, the simulated soil water contents exhibited large variation throughout the crop seasons, increasing soil water to values close to saturation during irrigation events, and then gradually decreasing due to percolation and root water uptake. Darouich et al. (2020) had already reported a similar soil moisture behavior in zucchini squash furrow irrigation treatments implemented in an adjacent experimental field.

In T1, the seasonal irrigation depths ranged from 219 to 421 mm (Table 3). In this drip treatment, triggering irrigation when soil water contents dropped below 90% of θ_{FC} produced the highest irrigation frequency (11–18 events) and the lowest depths per event (11–30 mm). Contrastingly, irrigation in T2, triggered when soil water contents dropped below 80% of θ_{FC}, resulted in larger depths per event (10–43 mm) but fewer events (10–13 events) than in T1. The seasonal irrigation depths were the lowest, ranging from 200 to 393 mm (Table 3). Nevertheless, both T1 and T2 used 57–64% less water than T0 due to the characteristics of the drip irrigation method used. In these treatments, the simulated soil water contents exhibited also less variation than in T0, with values remaining always close to or slightly below θ_{FC} but never approaching saturation.

The SIMDualKc model was able to reproduce field measurements reasonably well during the 2018 calibration season, with goodness-of-fit

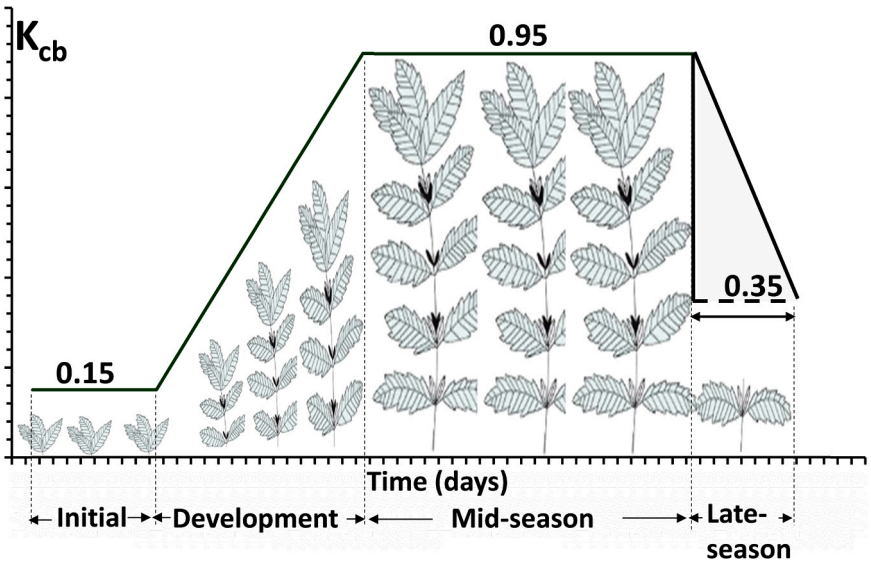

Fig. 3. Conceptual scheme of the basal crop coefficient (K_{cb}) for jute mallow during the four crop growth stages (the area in grey will depend on the length of the late season stage).

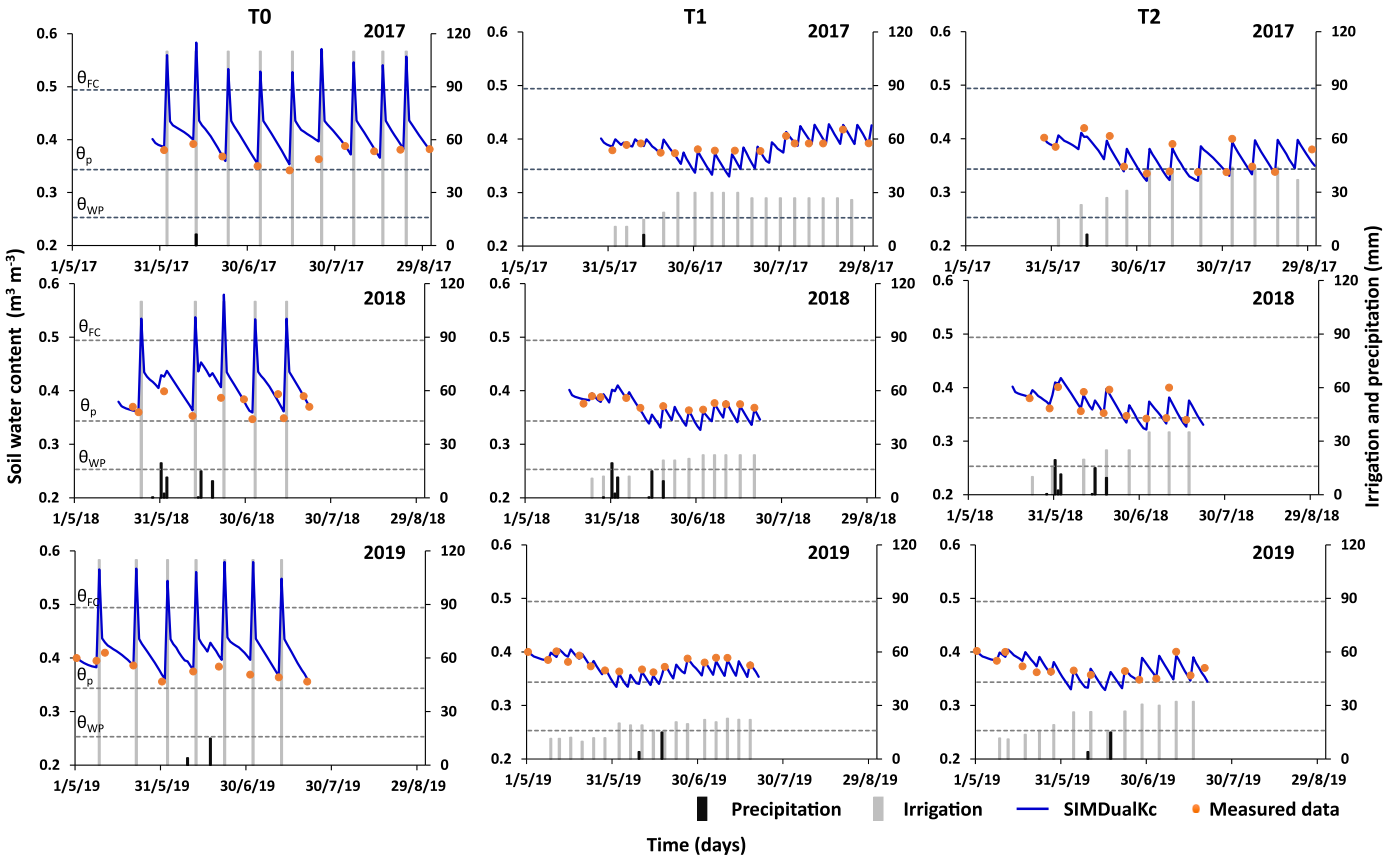

Fig. 4. Measured and simulated soil water contents in basin (T0) and drip (T1, T2) irrigation treatments during the 2017–2019 growing seasons (θ_{FC}, θ_{WP}, and θ_p correspond to soil water contents at field capacity, the wilting point, and at the depletion fraction for no stress).

Table 7
Goodness-of-fit indicators relative to calibration (2018) and validation (2017 and 2019) of soil water content simulations.

Year	Treatment	b_0 (-)	R^2 (-)	RMSE (m^3 m^{-3})	NRMSE (-)	PBIAS (%)	NSE (-)
2017 Validation	T0	1.021	0.667	0.0005	0.0014	-2.155	0.368
	T1	1.001	0.908	0.0002	0.0004	-0.098	0.710
	T2	0.971	0.938	0.0007	0.0018	2.866	0.812
2018 Calibration	T0	1.016	0.687	0.0007	0.0016	-1.648	0.468
	T1	0.998	0.790	0.0001	0.0002	0.187	0.690
	T2	0.985	0.892	0.0004	0.0011	1.551	0.790
2019 Validation	T0	1.023	0.690	0.0007	0.0018	-2.331	0.358
	T1	0.997	0.827	0.0001	0.0003	0.258	0.811
	T2	0.998	0.806	0.0003	0.0007	0.199	0.793

T0, T1, T2, experimental treatments; b_0, regression coefficient; R^2, coefficient of determination; RMSE, root mean square error; NRMSE, ratio of the RMSE to the standard deviation of observed data; PBIAS, percent bias; NSE, model efficiency.

indicating a quite good performance of the model (Table 7). These indicators showed a higher accuracy of soil water content simulations in the case of drip irrigation, T1 and T2, than with surface irrigation, in T0. The R^2 values were 0.79 and 0.89 in T1 and T2, respectively, while in T0 the R^2 value was 0.687. Nevertheless, all R^2 values were high enough to express the model's capability in explaining most of the variability of the observed data in the different treatments. Also, the NSE value was found to be superior in T1 and T2 (NSE of 0.69 and 0.79) than in T0 (NSE = 0.47), which still indicated that the residual variance was much smaller than the measured data variance in all treatments. Furthermore, the error of the estimate was generally quite small, resulting in RMSE and NRMSE values lower than 0.001 m^3 m^{-3} and 0.002, respectively. Lastly, both b_0, always close to 1.0, and PBIAS, quite small, did not allow finding a tendency for observations to be under- or over-predicted, thus confirming the goodness of the model simulations.

The parameters calibrated in 2018 were validated with the field data of the 2017 and 2019 growing seasons. The resulting goodness-of-fit indicators demonstrate a behavior of the SIMDualKc model similar to that of calibration in predicting soil water contents during those seasons. The goodness-of-fit indicators are also within the range of values reported in other successful SIMDualKc applications to vegetables (Zhang et al., 2018; Patil and Tiwari, 2019; Darouich et al., 2020), and well confirm the reliability of model simulations.

3.3. Standard and actual crop coefficients

Fig. 5 presents the seasonal values of the potential non-stressed basal crop coefficients (K_{cb}), the actual basal crop coefficients ($K_{cb\ act}$), the soil

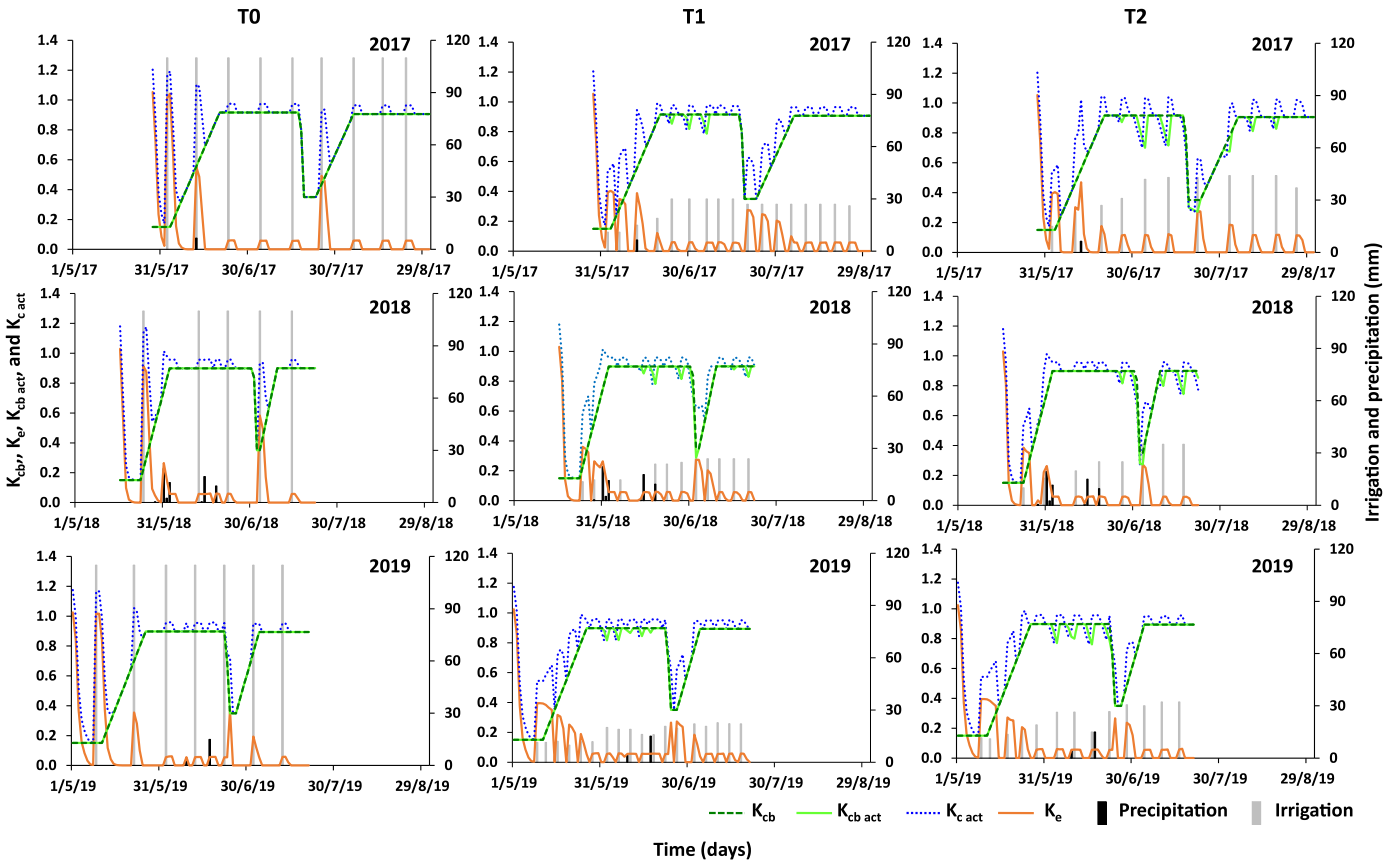

Fig. 5. Seasonal variation of the standard (non-stressed) basal crop coefficient (K_{cb}), the actual basal crop coefficient ($K_{cb\ act}$), the evaporation coefficient (K_e), and the actual crop coefficient ($K_{c\ act} = K_{cb\ act} + K_e$) in basin (T0) and drip (T1, T2) irrigation treatments during the 2017–2019 growing seasons, including the respective data on irrigation and precipitation.

evaporation coefficients (K_e), and the actual crop coefficients ($K_{c\ act} = K_{cb\ act} + K_e$) computed by SIMDualKc for jute mallow during the 2017–2019 growing seasons. Also included are the rainfall and irrigation events. As referred earlier, the K_{cb} values for the different crop stages were first calibrated from field data, and then further adjusted to local weather conditions following Allen et al. (1998) and Pereira et al. (2021). Hence, during the 2018 growing season, the $K_{cb\ ini}$, $K_{cb\ mid}$, and $K_{cb\ end}$ values were calibrated to 0.15, 0.95, and 0.95, respectively, for the first cut cycle, and to 0.35, 0.95, and 0.95, respectively, for the second cut cycle (Table 6). After adjustment to local weather conditions, the K_{cb} values varied slightly, with $K_{cb\ mid}$ and $K_{cb\ end}$ adjusting to near 0.90 during both cycles. The calibrated K_{cb} values were then validated during the 2017 and 2019 growing seasons. In 2017, the K_{cb} adjustment to local weather conditions resulted in $K_{cb\ mid}$ and $K_{cb\ end}$ values of 0.92 for the first cut cycle and 0.91 for the second cut cycle. In 2019, the adjusted values for $K_{cb\ mid}$ and $K_{cb\ end}$ were 0.90 and 0.89 for the first and second cut cycles, respectively.

In T0, the $K_{cb\ act}$ values always matched the potential standard K_{cb} ones. No water stress was ever observed during the three growing seasons (Fig. 5). However, the same was not true for T1 and T2, with the $K_{cb\ act}$ values occasionally departing from the K_{cb} curves during the mid-season when the frequency of irrigation was sub-optimal. Nevertheless, the water stress periods were always short, with the K_{cb} values equaling again the potential values after a successive irrigation or rain event.

The K_e values showed a contrasting behavior between basin and drip treatments, which was consistent throughout the three growing seasons. The K_e values started always high in all treatments after irrigation was applied to aid germination. Then, those values rapidly decreased due to the depletion of the evaporation soil layer. In T0, the K_e values were raised again to maximum values after the first irrigation event due to the increase of soil moisture in the surface soil layer. As jute mallow rapidly developed and the canopy fully covered soil surface reducing the amount of energy available for evaporation, the K_e values dropped to practically nil values during the rest of the growing season, only increasing with irrigation but always producing small peaks. The exception was the period after the first cut when the K_e values were raised again with the increase of the energy available for evaporation at the soil surface.

In T1 and T2, contrarily to T0, the K_e values never increased to maximum values after irrigation started. This occurred because irrigation depths and the f_w value in these treatments were much smaller than in T0, which prevented the K_e values to increase above 0.4. Since irrigation depths in both T1 and T2 were always enough to moist the soil evaporation layer, no differences were found in the K_e values except for those related to the dates of irrigation events and irrigation frequency. With the development of the plant's canopy, low K_e values were maintained for longer periods in T1 due to the higher irrigation frequency recorded in that treatment compared to T2. In both treatments, the K_e values eventually dropped to null values a few days after irrigation events, but more regularly in T2. Larger K_e values were also observed in both T1 and T2 after the first cut. However, K_e values remained always smaller than in T0 since irrigation depths and f_w were also smaller.

The $K_{c\ act}$ curve described the same trends observed for $K_{cb\ act}$ and K_e, clearly distinguishing the stages where crop transpiration and soil evaporation contributed most to crop evapotranspiration.

3.4. Soil water balance

Table 8 presents the soil water balance computed by SIMDualKc for

Table 8
Components of the annual soil water balance (values in brackets correspond to the percentage of the output in relation to the total water input).

Year	Treatment	Input				Output					
		I (mm)	Net P (mm)	ΔSW (mm)	Total (mm)	T_c (mm)	$T_{c\ act}$ (mm)	$T_{c\ act}/T_c$ (-)	E_s (mm)	DP (mm)	RO (mm)
2017	T0	990	6	12	1008	404	404 (40.1)	1.00	47 (4.7)	565 (56.1)	0 (0)
	T1	421	6	19	446	404	401 (89.9)	0.99	51 (11.4)	0 (0)	0 (0)
	T2	393	6	31	430	404	394 (91.6)	0.98	37 (8.6)	0 (0)	0 (0)
2018	T0	550	59	5	614	284	284 (46.3)	1.00	38 (6.2)	300 (48.9)	0 (0)
	T1	219	59	33	311	284	280 (90.0)	0.99	31 (10.0)	0 (0)	0 (0)
	T2	200	59	43	302	284	277 (91.7)	0.98	33 (10.9)	0 (0)	0 (0)
2019	T0	805	19	25	849	313	313 (36.9)	1.00	40 (4.7)	501 (59.0)	0 (0)
	T1	308	19	30	357	313	312 (87.4)	1.00	51 (14.3)	0 (0)	0 (0)
	T2	291	19	36	346	313	309 (89.3)	0.99	42 (12.1)	0 (0)	0 (0)

T0, T1, T2, experimental treatments; I, irrigation; P, precipitation; ΔSW, soil water storage variation; T_c, potential transpiration; $T_{c\ act}$, actual transpiration; E_s, actual evaporation; DP, deep percolation; RO, runoff.

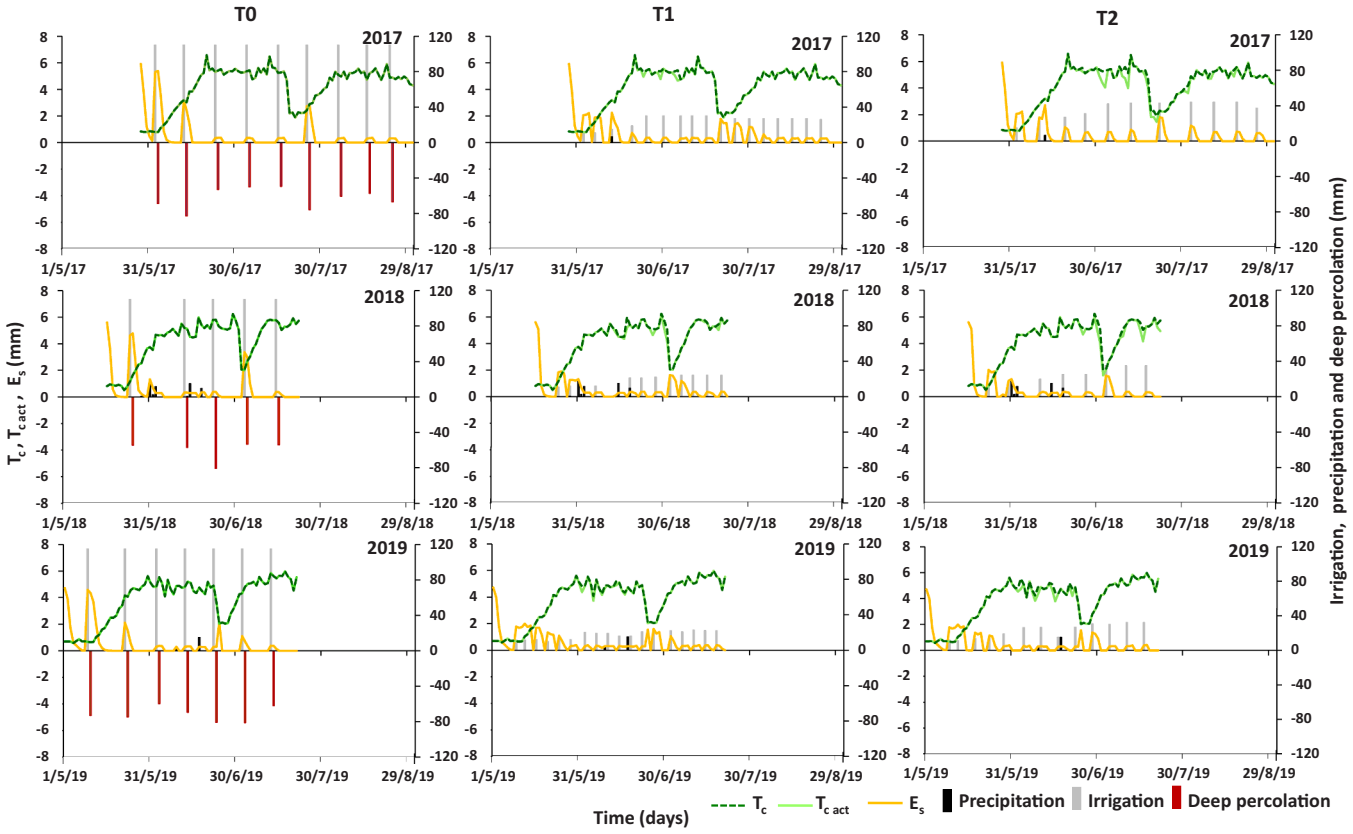

Fig. 6. Seasonal variation of daily potential crop transpiration (T_c), actual crop transpiration ($T_{c\ act}$), and soil evaporation (E_s) in basin (T0) and drip (T1, T2) irrigation treatments during the 2017–2019 growing seasons.

jute mallow during the 2017–2019 growing seasons. The length of the crop cycle decisively influenced the seasonal T_c, which values ranged from 284 to 404 mm. The lowest value was obtained in 2018, during a season that lasted 68 days. The highest was reached in 2017 when the crop season length was 96 days. The $T_{c\ act}/ET_{c\ act}$ ratio, which ranged from 0.86 to 0.91, showed the dominance of the transpiration component in seasonal ET values. As mentioned earlier, the $K_{cb\ act}$ values in T0 always matched the potential ones. As such, the $T_{c\ act}$ values also equaled the respective T_c values, meaning that no root water uptake reductions due to water stress were ever registered in this treatment (Fig. 6). The same was also observed for the drip treatments since the previously noticed departure between $K_{cb\ act}$ and K_{cb} values resulted only in meaningless reductions of the T_c values (2%). This was important to know since water stress can have a detrimental effect on jute mallow yields by reducing photosynthesis, respiration, and ultimately leaves growth.

Soil evaporation exhibited the same trends already described for the K_e values (Fig. 6), with higher rates during the initial crop stages and following the first cut. The seasonal soil evaporation was relatively low due to the fast crop growth, determining that full coverage of the soil surface by crop leaves (f_c = 0.95) was attained quite rapidly, thus limiting the energy available for evaporation. The seasonal E_s values ranged from 31 to 51 mm and were generally higher in T1 due to the higher irrigation frequency adopted in this treatment. The seasonal $ET_{c\ act}$ values ranged from 310 to 452 mm, which values are comparable with those reported by Odofin et al. (2011), 326–374 mm.

Deep percolation was only found in T0, with extremely large cumulated values (300–565 mm), which represented 55–62% of the irrigation water applied and 49–59% of the total water inputs (including rain and soil water storage). Contrastingly, crop water used in T1 ranged from 87% to 90% and in T2 from 89% to 92% in relation to the total water inputs. These results further reveal the inefficiency of the

traditional irrigation methods considered in this treatment. Traditional basin irrigation often results in high DP values due to the commonly low performance of these methods (Walker and Skogerboe, 1987; Darouich et al., 2012). However, many studies demonstrate that the performance of surface irrigation may be highly improved when design considers the appropriate relationships among the field size, slope, infiltration characteristics, inflow rates, and irrigation timing, duration, and frequency as already demonstrated for Syria (Darouich et al., 2012, 2014). While for the case study area, the percolated water ended up being collected by the drainage network system and delivered to the local stream to be eventually reused further downstream, in most Syrian irrigated areas those losses constitute an important contribution to groundwater recharge (Darouich et al., 2014). Thus, despite less efficient than the drip methods, the traditional surface irrigation method may well be a valuable mechanism for increasing the soil water storage to be used in irrigation.

3.5. Yield and water productivity indicators

Table 9 presents jute mallow yields measured in each treatment during the three growing seasons, as well as the respective water productivity indicators: WP_{WU}, WP_{Irrig}, WP_{ET}, WP_T, EWP, and EWPR indicators. Table 10 then presents the ANOVA table with the analysis of variance for the effects of treatments and seasons on jute mallow yields and WP indicators. Jute mallow yields were always higher in T1 and T2 than in T0. In T1, yields averaged 16.31 Mg ha^{-1}, with annual maximum and minimum values of 18.34 and 13.20 Mg ha^{-1}, respectively. In T2, the yield average was only slightly below the previous one (15.20 Mg ha^{-1}), with yearly values ranging from 14.73 to 15.59 Mg ha^{-1}. The first cut was always more productive than the second. Contrastingly, yields in T0 averaged only 11.07 Mg ha^{-1}, with yearly values also ranging from 10.42 to 11.94 Mg ha^{-1}. Statistics showed that the difference in the average between treatments was significant at the 99.9% level of confidence, but no relation was found either for the growing seasons or the interaction of both factors (i.e., years × treatments).

Literature is quite scarce on the effect of irrigation method and scheduling on jute mallow yields. Yousef et al. (2020) reported a maximum yield of 8.0 Mg ha^{-1} in well fertilized treatments irrigated every ten days by flooding in the Assiut governorate, Central Egypt, during the 2017 and 2018 growing seasons. Asmaa et al. (2014) also presented yields ranging from 10.48 to 12.87 Mg ha^{-1} for jute mallow irrigated by drip in the Beheira Governorate, Northern Egypt, during the 2010 and 2011 growing seasons. The previous values were smaller than those obtained in this study. Yet, as in this study, crop irrigation by traditional methods always returned the lowest marketable yields. The same had already been observed in Darouich et al. (2020) for zucchini squash. Like then for traditional furrows, basin irrigation resulted in high percolation losses, which most certainly promoted nutrient leaching and reduced nutrient availability for jute mallow growth.

Drip irrigation treatments also returned higher water productivity indicators than the basin irrigation treatment (Table 9). This trend was noticed not only when analyzing the absolute values of each indicator, but also their yearly variation assuming always the respective WP_{WU} values as the baseline. As a result, the WP_{irrig} values showed a greater increase in the drip treatments (6–50%) than in T0 (2–11%) when considering WP_{WU} as the calculation basis, thus revealing the higher efficiency of the drip irrigation system. On the other hand, no substantial differences were found between WP_{WU} and WP_{ET} in the drip treatments, contrarily to T0 where this indicator increased by 91–140%, thus meaning that most of the water inputs in T1 and T2 were used in the ET process (i.e., no percolation or runoff occurred). A similar analysis was drawn for WP_T, but here values in the drip treatments suffered a slight increase (8–15%) when compared to WP_{ET} because evaporation was then not considered.

The WP_{WU} and WP_{irrig} showed significant differences in the average between treatments and between years at the 99.9% level of confidence, but no differences were found for interaction between both factors (Table 10). Likewise, the WP_{ET} and WP_T showed contrasting differences between treatments and between years, but the level of confidence was smaller than in the previous indicators (99%). Also, the economical indicators were more advantageous in the drip treatments than in the basin treatment, with the average values of both indicators being again found to be significantly different for treatments and years at the 99.9% level of confidence. The EWP values ranged from 0.8 to 1.3 \$ m^{-3} in T1 and T2 while they varied only from 0.24 to 0.43 \$ m^{-3} in T0. On the other hand, the EWPR values ranged from 15.87 to 33.51 in T1 and T2, while in T0 they reached 4.39–8.68. The EWPR values for jute mallow were thus smaller than those in Darouich et al. (2020) for zucchini squash, which ranged from 14.3 to 23.9 in the furrow treatment and from 24.5 to 90.0 in the drip treatments. Therefore, jute mallow may be considered a less interesting crop to be grown in the Akkar plain, Syria, but valuable enough to be included in a crop rotation scheme.

3.6. Defining irrigation thresholds

Fig. 7 presents NIR of jute mallow for scenarios AI, AII, BI, and BII for the period 1998–2020. For scenario AI, which considered May 1st as the sowing date, the dates of the crop stages based on the GDD, and basin irrigation, the NIR values ranged from 314 to 397 mm. Yet, no substantial differences were found for 21 of the 23 years, in which NIR values varied only from 386 to 397 mm. Therefore, NIR values corresponding to this scenario in Fig. 7 were practically constant. This was

Table 9
Yield and water productivity indicators.

Year	Treatment	Yield (Mg ha^{-1})			WP_{WU} (kg m^{-3})	WP_{Irrig} (kg m^{-3})	WP_{ET} (kg m^{-3})	WP_T (kg m^{-3})	EWP (\$ m^{-3})	EWPR (-)
		1^{st} cut	2^{nd} cut	Total						
2017	T0	7.00	3.86	10.86	1.08	1.10	2.41	2.69	0.24	4.39
	T1	11.20	6.18	17.38	3.90	4.13	3.84	4.33	0.86	16.52
	T2	11.19	4.40	15.59	3.62	3.97	3.57	3.96	0.80	15.87
2018	T0	8.34	3.60	11.94	1.95	2.17	3.72	4.21	0.43	8.68
	T1	11.14	7.20	18.34	5.92	8.38	5.77	6.56	1.30	33.51
	T2	9.73	5.00	14.73	4.90	7.35	4.77	5.31	1.08	29.41
2019	T0	6.90	3.52	10.42	1.23	1.29	2.95	3.33	0.27	5.18
	T1	8.30	4.90	13.20	3.70	4.29	3.64	4.24	0.81	17.15
	T2	9.70	5.58	15.28	4.42	5.25	4.36	4.94	0.97	21.01

WP_{WU}, total water productivity; WP_{irrig}, irrigation water productivity; WP_{ET}, consumptive use water productivity; WP_T, transpiration water productivity; EWP, economic water productivity; EWPR, economic water productivity ratio.

Table 10
Analysis of variance of measured jute mallow yields and water productivity indicators.

Source of variation	Degrees of freedom	Sum of squares	Mean square	F	P
Total yield					
Years	2	28.02	14.01	1.45	0.252
Treatments	2	182.46	91.23	9.45	0.001**
Years x Treatments	4	38.18	9.55	0.99	0.430
Error	27	260.60	9.65		
WP_{WU}					
Years	2	13.20	6.60	10.53	0.000***
Treatments	2	72.00	36.00	57.42	0.000***
Years x Treatments	4	4.00	1.00	1.60	0.204
Error	27	16.93	0.63		
WP_{Irrig}					
Years	2	56.99	28.50	27.98	0.000***
Treatments	2	130.71	65.36	64.18	0.000***
Years x Treatments	4	15.28	3.82	3.75	0.015*
Error	27	27.50	1.02		
WP_{ET}					
Years	2	14.26	7.13	9.32	0.001**
Treatments	2	13.66	6.83	8.93	0.001**
Years x Treatments	4	3.18	0.82	1.07	0.389
Error	27	20.65	0.77		
WP_T					
Years	2	18.26	9.13	9.36	0.001**
Treatments	2	18.10	9.05	9.27	0.001**
Years x Treatments	4	4.11	1.03	1.05	0.399
Error	27	26.36	0.98		
EWP					
Years	2	0.64	0.32	10.53	0.000***
Treatments	2	3.49	1.74	57.42	0.000***
Years x Treatments	4	0.19	0.05	1.60	0.204
Error	27	0.82	0.03		
EWPR					
Years	2	911.89	455.94	27.98	0.000***
Treatments	2	2091.39	1045.70	64.18	0.000***
Years x Treatments	4	244.52	61.13	3.75	0.015*
Error	27	439.93	16.29		

Significant levels: 0*** 0.001** 0.05*
WP_{WU}, total water productivity; WP_{irrig}, irrigation water productivity; WP_{ET}, consumptive use water productivity; WP_T, transpiration water productivity; EWP, economic water productivity; EWPR, economic water productivity ratio.

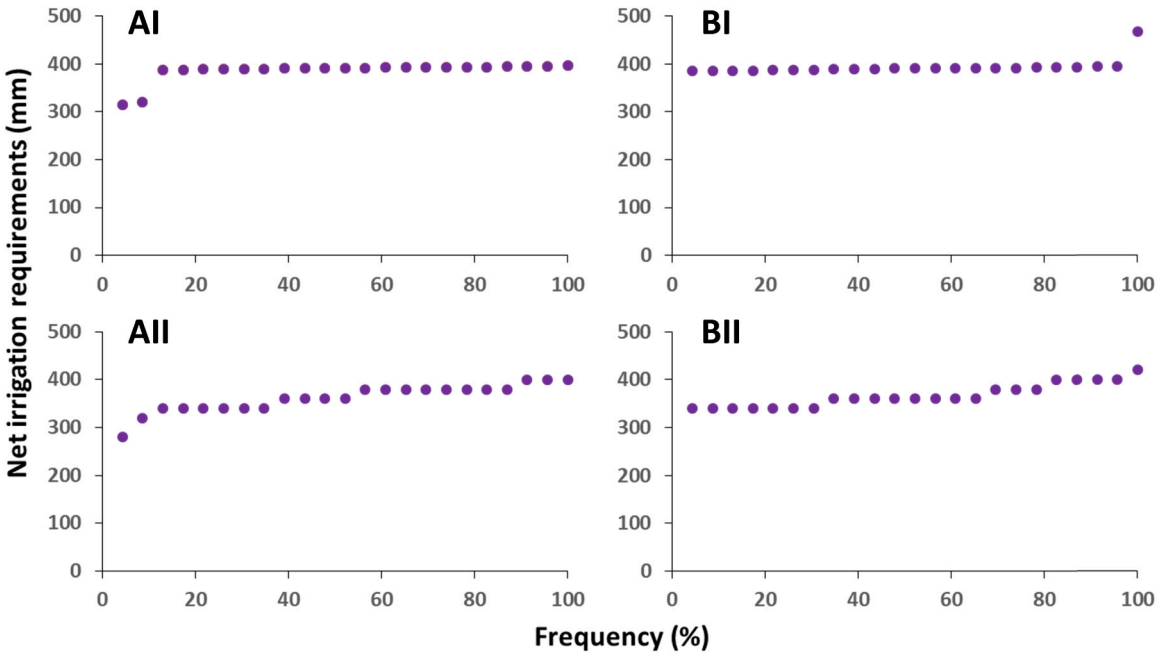

Fig. 7. Frequency distribution of the net irrigation requirements for Jute mallow, Akkar plain, Syria, relative to the time period of 1998–2020. A and B refer to scenarios with different sowing dates. I and II refer to scenarios with different irrigation methods (I, basin irrigation; II, drip irrigation).

Table 11
Soil water balance for the years representing average, high, and very high water demand in different scenarios.

Scenario	Water demand	Year	ΔSW (mm)	Net P (mm)	I (mm)	T_c (mm)	$T_{c\ act}$ (mm)	E_s (mm)	DP (mm)
AI	Average	2019	-25	19	392	364	363	28	0
	High	2010	3	3	393	385	383	21	0
	Very high	2020	-2	0	395	381	380	18	0
BI	Average	2000	-21	0	391	350	349	26	0
	High	2013	-31	0	393	344	343	24	0
	Very high	2019	0	19	395	380	379	22	20
AII	Average	2005	37	19	360	379	376	45	0
	High	2015	40	17	380	410	406	36	0
	Very high	2009	25	5	400	399	395	41	0
BII	Average	2012	25	0	360	361	356	35	0
	High	2009	20	0	400	394	390	37	0
	Very high	2017	37	6	400	403	399	51	0

ΔSW, soil water storage variation; P, precipitation; I, irrigation; T_c, potential transpiration; $T_{c\ act}$, actual transpiration; E_s, actual evaporation; DP, deep percolation. A and B refer to scenarios with different sowing dates. I and II refer to scenarios with different irrigation methods (I, basin irrigation; II, drip irrigation).

explained by the small interannual variation of the atmospheric demand during the crop cycle, the commonly adopted irrigation trigger threshold (MAD = p), and the high irrigation depths applied in each event to refill the soil water contents to field capacity, which were not sensitive to small variations on atmospheric demand during the 23-year period. The same results were observed for scenario BI, which considered the same irrigation method, but in this case, the sowing date and the crop growth stages were defined as in 2017. NIR ranged from 386 to 395 mm for 22 of the 23 years, with only one season requiring an extra irrigation event that increased NIR to 468 mm.

For scenario AII, which considered the same assumptions as AI but drip irrigation, NIR ranged from 280 to 400 mm. For scenario BII, also with drip irrigation, NIR values varied from 340 to 420 mm despite the noticed small interannual variation of the atmospheric demand during the crop cycle. The introduction of drip irrigation allowed to better distinguish NIR of jute mallow along the seasons. Nonetheless, NIR variation in these scenarios was relatively narrow, but with values being always similar or lower than those computed in the basin irrigation scenarios.

Table 11 presents the soil water balance for the years representing the average, high, and very high demand, which corresponded to the probabilities of 50%, 80%, and 95% for non-exceedance when assuming a normal distribution for the 1998–2020 NIR time series, that were always different for each scenario. For scenarios AI and BI, as referred above, no substantial differences were found in the NIR of jute mallow. Nonetheless, T_c and $T_{c\ act}$ values increased as expected from the years representing average water demand to the years representing very high water demand. For scenarios AII and BII, the increase of NIR was followed by an increase of T_c and $T_{c\ act}$ values, confirming the capability of drip irrigation schemes to save water not just due to the greater efficiency of these systems, but also because with drip irrigation it is easier to adjust irrigation depths to atmospheric demand.

4. Conclusions

The modernization of irrigation methods and practices in the Syrian Akkar Plain has provided the context for this research, in which irrigation requirements of jute mallow (*Corchorus olitorius* L.) were investigated. The SIMDualKc model, which follows the FAO56 dual-K_c approach, was used to compute the soil water balance in jute mallow plots irrigated with basin and drip irrigation methods during three growing seasons (2017–2019). The model successfully simulated soil

water contents in diverse experimental plots, with the level of agreement between measured and simulated data returning RMSE values lower than 0.001 $m^3 m^{-3}$ and NSE values ranging from 0.36 to 0.81. The calibrated basal crop coefficients (K_{cb}) were 0.15, 0.95, and 0.95 for the initial ($K_{cb\ ini}$), mid-season ($K_{cb\ mid}$), and end-season ($K_{cb\ end}$) stages, respectively, which should be considered when computing future crop irrigation needs in the Syrian Akkar Plain. The corresponding standard K_{cb} values to be used worldwide and adjusted to local climates are, for the first cut cycle, $K_{cb\ ini} = 0.15$, $K_{cb\ mid} = 0.92$, and $K_{cb\ end} = 0.90$, and for the second cycle, $K_{cb\ ini} = 0.35$, $K_{cb\ mid} = 0.91$, and $K_{cb\ end} = 0.90$.

Jute mallow yields were significantly higher in the drip irrigation treatments than in the basin treatment, with the water productivity and economic indicators responding also positively to water savings generated by the higher application efficiency of the drip systems through the highly frequent application of small irrigation depths that better adjust to the crop water demand.

The net irrigation requirements were also investigated using the SIMDualKc model over a long time period of 23 years (1998–2020), where the probabilities of the demand for irrigation water were assessed in scenarios considering different crop season lengths, irrigation methods, and application depths and schedules. Except for the extremes of the long-term weather time series, the probability of the demand for irrigation water for the years representing the average, high, and very high demand, which correspond respectively to the probabilities of 50%, 80%, and 95% for non-exceedance, were relatively similar for the basin irrigation scenarios (from 391 to 395 mm) but more distinct for drip irrigation scenarios (from 360 to 400 mm), further showing the advantages of this irrigation method to save water.

Declaration of Competing Interest

The authors declare that they have no known competing financial interests or personal relationships that could have appeared to influence the work reported in this paper.

Acknowledgments

LEAF and MARETEC acknowledge national funds from Fundação para a Ciência e Tecnologia through Projects UID/AGR/04129/2020 and UIDB/50009/2020, respectively. H. Darouich and T.B. Ramos were supported by contracts CEECIND/01153/2017 and CEECIND/01152/2017, respectively.

References

Abou Zakhem, B., Hafez, R., 2007. Environmental isotope study of seawater intrusion in the coastal aquifer (Syria). Environ. Geol. 51 (8), 1329–1339. https://doi.org/10.1007/s00254-006-0431-x.

Abou Zakhem, B., Al Ain, F., Hafez, R., 2019. Assessment of field water budget components for increasing water productivity under drip irrigation in arid and semi-arid areas, Syria. Irrig. Drain. 68 (3), 452–463. https://doi.org/10.1002/ird.2286.

Allen, R.G., Pereira, L.S., Raes, D., Smith, M., 1998. Crop Evapotranspiration. Guidelines for Computing Crop Water Requirements. FAO Irrig. Drain. FAO, Rome, p. 300. Paper 56.

Allen, R.G., Pereira, L.S., Smith, M., Raes, D., Wright, J.L., 2005. FAO-56 dual crop coefficient method for estimating evaporation from soil and application extensions. J. Irrig. Drain. Eng. 131, 2–13. https://doi.org/10.1061/(ASCE)0733-9437(2005)131:1(2).

Allen, R.G., Pereira, L.S., 2009. Estimating crop coefficients from fraction of ground cover and height. Irrig. Sci. 28 (1), 17–34. https://doi.org/10.1007/s00271-009-0182-z.

Allen, R.G., Pereira, L.S., Howell, T.A., Jensen, M.E., 2011a. Evapotranspiration information reporting: I. Factors governing measurement accuracy. Agric. Water Manag. 98 (6), 899–920. https://doi.org/10.1016/j.agwat.2010.12.015.

Allen, R.G., Pereira, L.S., Howell, T.A., Jensen, M.E., 2011b. Evapotranspiration information reporting: II. Recommended documentation. Agric. Water Manag. 98 (6), 921–929. https://doi.org/10.1016/j.agwat.2010.12.016.

Asmaa, R.M., Hafez, M.M., Shafeek, M.R., Aisha, H.A., 2014. Growth, yield and leaf content of Jews mallow plant (Corchorus olitorius) by soil fertilizer with different level of compost manure and chemical fertilizer. Middle East J. Agric. Res. 3 (3), 543–548.

CAPMAS, 2020, Central Agency for Public Mobilization and Statistics. Cairo, Egypt. ⟨https://www.capmas.gov.eg/HomePage.aspx⟩ (Last accessed 19 November 2020).

CBS, 2019, Agriculture. Central Bureau of Statistics, Chapter 4. Tables 7 and 10, Damascus, Syria. ⟨http://cbssyr.sy/index-EN.htm⟩ (Last accessed 28 December 2020).

Chard, E.D., 1981, An Economic Analysis of the Akkar Plain Project. Utah State University, All Graduate Theses and Dissertations. Paper 4210.

Choudhary, S.B., Sharma, H.K., Karmakar, P.G., Kumar, A.A., Saha, A.R., Hazra, P., Mahapatra, B.S., 2013. Nutritional profile of cultivated and wild jute (Corchorus) species. Aust. J. Crop Sci. 7 (13), 1973–1982.

Dane, J.H., Hopmans, J.W., 2002. Pressure plate extractor. In: Dane, J.H., Topp, G.C. (Eds.), Methods of Soil Analysis, Part 4, Physical Methods. Soil Science Society of America Book Series. Soil Science Society of America, Madison, Wisconsin, pp. 688–690.

Darouich, H., Gonçalves, J.M., Muga, A., Pereira, L.S., 2012. Water saving vs. farm economics in cotton surface irrigation: an application of multicriteria analysis. Agric. Water Manag. 115, 223–231. https://doi.org/10.1016/j.agwat.2012.09.006.

Darouich, H., Pedras, C.M.G., Gonçalves, J.M., Pereira, L.S., 2014. Drip vs. surface irrigation: a comparison focusing water saving and economic returns using multicriteria analysis applied to cotton. Biosyst. Eng. 122, 74–90. https://doi.org/10.1016/j.biosystemseng.2014.03.010.

Darouich, H., Cameira, R.M., Gonçalves, J.M., Paredes, P., Pereira, L.S., 2017. Comparing sprinkler and surface irrigation for wheat using multi-criteria analysis: water saving vs. economic returns. Water 9 (1), 50. https://doi.org/10.3390/w9010050.

Darouich, H., Karfoul, R., Eid, H., Ramos, T.B., Baddour, N., Moustafa, A., Assaad, M.I., 2020. Modeling zucchini squash irrigation requirements in the Syrian Akkar region using the FAO56 dual-Kc approach. Agric. Water Manag. 229, 105927 https://doi.org/10.1016/j.agwat.2019.105927.

Fader, M., Shi, S., von Bloh, W., Bondeau, A., Cramer, W., 2016. Mediterranean irrigation under climate change: more efficient irrigation needed to compensate increases in irrigation water requirements. Hydrol. Earth Syst. Sci. Discuss. 20, 953–973. https://doi.org/10.5194/hess-20-953-2016.

FAO/IIASA/ISRIC/ISS-CAS/JRC, 2009, Harmonized World Soil Database (version 1.1). FAO, Rome, Italy, and IIASA, Laxenburg, Austria.

Fernández, J.E., Alcon, F., Diaz-Espejo, A., Hernandez-Santana, V., Cuevas, M.V., 2020. Water use indicators and economic analysis for on-farm irrigation decision: a case study of a super high density olive tree orchard. Agric. Water Manag. 237, 106074 https://doi.org/10.1016/j.agwat.2020.106074.

Fondio, L., Grubben, G.J.H., 2011. In: Brink, M., Achigan-Dako, E.G. (Eds.), Corchorus olitorius L. Plant Resources of Tropical Africa (PROTA), Wageningen, Netherlands https://uses.plantnet-project.org/en/Corchorus_olitorius_%28PROTA%29 (Last accessed 20.11.2020).

Giménez, L., García-Petillo, M., Paredes, P., Pereira, L.S., 2016. Predicting maize transpiration, water use and productivity for developing improved supplemental irrigation schedules in western Uruguay to cope with climate variability. Water 8, 309. https://doi.org/10.3390/w8070309.

González, M.G., Ramos, T.B., Carlesso, R., Paredes, P., Petry, M.T., Martins, J.D., Aires, N.P., Pereira, L.S., 2015. Modelling soil water dynamics of full and deficit drip irrigated maize cultivated under a rain shelter. Biosyst. Eng. 132, 1–18. https://doi.org/10.1016/j.biosystemseng.2015.02.001.

IUSS Working Group WRB, 2014, World Reference Base for Soil Resources 2014. International Soil Classification System for Naming Soils and Creating Legends for Soil Maps. World Soil Resources Reports No. 106. FAO, Rome.

Janat, M., 2007. Efficiency of nitrogen fertilizer for potato under fertigation utilizing a nitrogen tracer technique. Commun. Soil Sci. Plant Anal. 38 (17–18), 2401–2422. https://doi.org/10.1080/00103620701588775.

Kool, D., Agam, N., Lazarovitch, N., Heitman, J.L., Sauer, T.J., Ben-Gal, A., 2014. A review of approaches for evapotranspiration partitioning. Agric. For. Meteorol. 184, 56–70. https://doi.org/10.1016/j.agrformet.2013.09.003.

Köppen, W., 1884. Die Wärmezonen der Erde, nach der Dauer der heissen, gemässigten und kalten Zeit und nach der Wirkung der Wärme auf die organische Welt betrachtet. Meteorol. Z. 1, 215–226.

Kumari, N., Choudhary, S.B., Sharma, H.K., Singh, B.K., Kumar, A.A., 2019. Health-promoting properties of Corchorus leaves: a review. J. Herb. Med. 15, 100240 https://doi.org/10.1016/j.hermed.2018.10.005.

Legates, D., McCabe, G., 1999. Evaluating the use of goodness of fit measures in hydrologic and hydroclimatic model validation. Water Resour. Res. 35, 233–241. https://doi.org/10.1029/1998WR900018.

Lin, L.J., Hsiao, Y.Y., Kuo, C.G., 2009, Discovering indigenous treasures: Promising indigenous vegetables from around the world. AVRDC – The World Vegetable Center Publication No. 09–720. AVRDC - The World Vegetable Center, Shanhua, Taiwan.

Liu, Y., Pereira, L.S., Fernando, R.M., 2006. Fluxes through the bottom boundary of the root zone in silty soils: parametric approaches to estimate groundwater contribution and percolation. Agric. Water Manag. 84, 27–40. https://doi.org/10.1016/j.agwat.2006.01.018.

López-Urrea, R., Martín de Santa Olalla, F., Montoro, A., López-Fuster, P., 2009. Single and dual crop coefficients and water requirements for onion (Allium cepa L.) under semiarid conditions. Agric. Water Manag. 96 (6), 1031–1036. https://doi.org/10.1016/j.agwat.2009.02.004.

Martins, J.D., Rodrigues, G.C., Paredes, P., Carlesso, R., Oliveira, Z.B., Knies, A.E., Petry, M.T., Pereira, L.S., 2013. Dual crop coefficients for maize in southern Brazil: model testing for sprinkler and drip irrigation and mulched soil. Biosyst. Eng. 115, 291–310. https://doi.org/10.1016/j.biosystemseng.2013.03.016.

Moriasi, D.N., Arnold, J.G., Van Liew, M.W., Bingner, R.L., Harmel, R.D., Veith, T.L., 2007. Model evaluation guidelines for systematic quantification of accuracy in

watershed simulations. Trans. ASABE 50, 885–900. https://doi.org/10.13031/2013.23153.
Mourad, K.A., Alshihabi, O., 2016. Assessment of future Syrian water resources supply and demand by the WEAP model. Hydrol. Sci. J. 61 (2), 393–401. https://doi.org/10.1080/02626667.2014.999779.
Nash, J.E., Sutcliffe, J.V., 1970. River flow forecasting through conceptual models: part 1. A discussion of principles. J. Hydrol. 10 (3), 282–290. https://doi.org/10.1016/0022-1694(70)90255-6.
Nelson, D.W., Sommers, L.E., 1982. Total carbon, organic carbon, and organic matter. In: Page, A.L. (Ed.), Methods of soil analysis. Part 2. Chemical and microbiological properties. Agron. Monogr. 9. ASA and SSSA, Madison, WI., pp. 539–579
Ngomuo, M.S., Stoilova, T., Feyissa, T., Kassim, N., Ndakidemi, P.A., 2017. Leaf and seed yield of jute mallow (*Corchorus olitorius* L.) accessions under field conditions for two consecutive growing seasons. J. Hortic. Sci. Biotechnol. 92 (6), 614–620. https://doi.org/10.1080/14620316.2017.1304168.
Odofin, A.J., Oladiran, J.A., Oladipo, J.A., Wuya, E.P., 2011. Determination of evapotranspiration and crop coefficients for bush okra (*Corchorus olitorius*) in a sub-humid area of Nigeria. Afr. J. Agric. Res. 6 (17), 3949–3953. https://doi.org/10.5897/AJAR10.812.
Oweis, T., Rodrigues, P.N., Pereira, L.S., 2003. Simulation of supplemental irrigation strategies for wheat in Near East to cope with water scarcity. In: Rossi, G., Cancelliere, A., Pereira, L.S., Oweis, T., Shatanawi, M., Zairi, A. (Eds.), Tools for Drought Mitigation in Mediterranean Regions. Kluwer, Dordrecht, pp. 259–272. https://doi.org/10.1007/978-94-010-0129-8_15.
Paço, T.A., Ferreira, M.I., Rosa, R.D., Paredes, P., Rodrigues, G.C., Conceição, N., Pacheco, C.A., Pereira, L.S., 2012. The dual crop coefficient approach using a density factor to simulate the evapotranspiration of a peach orchard: SIMDualKc model vs. Eddy covariance measurements. Irrig. Sci. 30 (2), 115–126. https://doi.org/10.1007/s00271-011-0267-3.
Palada, M.C., Chang, L.C., 2003. Suggested Cultural Practices for Jute Mallow. Asian Vegetable Research and Development Center, Shanhua, Taiwan.
Paredes, P., D'Agostino, D., Assif, M., Todorovic, M., Pereira, L.S., 2018a. Assessing potato transpiration, yield and water productivity under various water regimes and planting dates using the FAO dual Kc approach. Agric. Water Manag. 195, 11–24. https://doi.org/10.1016/j.agwat.2017.09.011.
Paredes, P., Rodrigues, G.J., Petry, M.T., Severo, P.O., Carlesso, R., Pereira, L.S., 2018b. Evapotranspiration partition and crop coefficients of tifton 85 bermudagrass as affected by the frequency of cuttings. Application of the FAO56 dual Kc model. Water 10, 558. https://doi.org/10.3390/w10050558.
Patil, A., Tiwari, K.N., 2019. Quantification of transpiration and evaporation of okra under subsurface drip irrigation using SIMDualKc model during vegetative development. Int. J. Veg. Sci. 25, 27–39. https://doi.org/10.1080/19315260.2018.1462875.
Pereira, L.S., Oweis, T., Zairi, A., 2002. Irrigation management under water scarcity. Agric. Water Manag. 57, 175–206. https://doi.org/10.1016/S0378-3774(02)00075-6.
Pereira, L.S., Cordery, I., Iacovides, I., 2009a. Coping with Water Scarcity. Addressing the Challenges. Springer, Dordrecht, p. 382.
Pereira, L.S., Paredes, P., Cholpankulov, E.D., Inchenkova, O.P., Teodoro, P.R., Horst, M. G., 2009b. Irrigation scheduling strategies for cotton to cope with water scarcity in the Fergana Valley, Central Asia. Agric. Water Manag. 96, 723–735. https://doi.org/10.1016/j.agwat.2008.10.013.
Pereira, L.S., Cordery, I., Iacovides, I., 2012. Improved indicators of water use performance and productivity for sustainable water conservation and saving. Agric. Water Manag. 108, 39–51. https://doi.org/10.1016/j.agwat.2011.08.022.
Pereira, L.S., Allen, R.G., Smith, M., Raes, D., 2015a. Crop evapotranspiration estimation with FAO56: past and future. Agric. Water Manag. 147, 4–20. https://doi.org/10.1016/j.agwat.2014.07.031.
Pereira, L.S., Paredes, P., Rodrigues, G.C., Neves, M., 2015b. Modeling malt barley water use and evapotranspiration partitioning in two contrasting rainfall years. Assessing AQUACROP and SIMDualKc models. Agric. Water Manag. 159, 239–254. https://doi.org/10.1016/j.agwat.2015.06.006.
Pereira, L.S., Paredes, P., Jovanovic, N., 2020a. Soil water balance models for determining crop water and irrigation requirements and irrigation scheduling focusing on the FAO56 method and the dual Kc approach. Agric. Water Manag. 241, 106357 https://doi.org/10.1016/j.agwat.2020.106357.
Pereira, L.S., Paredes, P., Melton, F., Johnson, L., Wang, T., López-Urrea, R., Cancela, J. J., Allen, R., 2020b. Prediction of crop coefficients from fraction of ground cover and height. Background and validation using ground and remote sensing data. Agric. Water Manag. 241, 106197 https://doi.org/10.1016/j.agwat.2020.106197.
Pereira, L.S., Paredes, P., López-Urrea, R., Hunsaker, D.J., Mota, M., Mohammadi Shad, Z., 2021. Standard single and basal crop coefficients for vegetable crops, an update of FAO56 crop water requirements approach. Agric. Water Manag. 243, 106196 https://doi.org/10.1016/j.agwat.2020.106196.
Ritchie, J.T., 1972. Model for predicting evaporation from a row crop with incomplete cover. Water Resour. Res. 8 (5), 1204–1213. https://doi.org/10.1029/WR008i005p01204.
Rosa, R.D., Paredes, P., Rodrigues, G.C., Alves, I., Fernando, R.M., Pereira, L.S., Allen, R. G., 2012a. Implementing the dual crop coefficient approach in interactive software. 1. Background and computational strategy. Agric. Water Manag. 103, 8–24. https://doi.org/10.1016/j.agwat.2011.10.013.
Rosa, R.D., Paredes, P., Rodrigues, G.C., Alves, I., Fernando, R.M., Pereira, L.S., Allen, R. G., 2012b. Implementing the dual crop coefficient approach in interactive software. 2. Model Test. Agric. Water Manag. 103, 62–77. https://doi.org/10.1016/j.agwat.2011.10.018.
Sadiddin, A., 2013. An assessment of policy impact on agricultural water use in the northeast of Syria. Environ. Dev. Sustain 2, 74–105. https://doi.org/10.5296/emsd.v2i1.3255.
Soil Survey Staff, 2011, Soil Survey Laboratory Information Manual; Soil Survey Investigations Report No. 45, Version 2.0. U.S. Department of Agriculture, Natural Resources Conservation Service, Washington, DC, USA.
USDA-SCS, 1972, National Engineering Handbook, Hydrology, Section 4. United States Department of Agriculture, Soil Conservation Service (Chapters 4–10).
Varela-Ortega, C., Sagardoy, J.A., 2003, Irrigation water policies in Syria: current developments and future options. In: Fiorillo, C., Vercueil, J. (Eds.), Syrian Agriculture at the Crossroads. FAO Agricultural Policy and Economic Development Series No. 8, Food and Agriculture Organization of the United Nations, Rome Chapter 13.
Walker, W.R., Skogerboe, G., 1987. Surface Irrigation: Theory and Practice. Prentice-Hall, Inc, Englewood Cliffs, New Jersey.
Wattenbach, H., 2006, Farming Systems of the Syrian Arab Republic. FAO Project GCP/SYR/006/ITA, the National Agricultural Policy Center (NAPC), Damascus, Syria.
Wei, Z., Paredes, P., Liu, Y., Chi, W.-W., Pereira, L.S., 2015. Modelling transpiration, soil evaporation and yield prediction of soybean in North China Plain. Agric. Water Manag. 147, 43–53. https://doi.org/10.1016/j.agwat.2014.05.004.
Yakoub, A.R.B., Abdehedi, O., Jridi, M., Elfalleh, W., Nasri, M., Ferchichi, A., 2018. Flavonoids, phenols, antioxidant, and antimicrobial activities in various extracts from Tossa jute leave (*Corchorus olitorius* L.). Ind. Crop Prod. 118, 206–213. https://doi.org/10.1016/j.indcrop.2018.03.047.
Yates, F., 1934. The analysis of multiple classifications with unequal numbers in the different classes. J. Am. Stat. Assoc. 29 (185), 51–66. https://doi.org/10.2307/2278459.
Yigezu, Y.A., Ahmed, M.A., Shideed, K., Aw-Hassan, A., El-Shater, T., 2013. Implications of a shift in irrigation technology on resources use efficiency: a Syrian case. Agric. Syst. 118, 14–22. https://doi.org/10.1016/j.agsy.2013.02.003.
Yousef, A.F., Youssef, M.A., Ali, M.M., Ibrahim, M.M., Xu, Y., Mauro, R.P., 2020. Improved growth and yield response of jew's mallow (*Corchorus olitorius* L.) plants through biofertilization under semi-arid climate conditions in Egypt. Agronomy 10, 1801. https://doi.org/10.3390/agronomy10111801.
Zakaria, Z., Somchit, M., Zaiton, H., Mat Jais, A., Sulaiman, M., Farah, W., Nazaratulmawarina, R., Fatimah, C., 2006. The in vitro antibacterial activity of *Corchorus olitorius* extracts. Int. J. Pharmacol. 2, 213–215. https://doi.org/10.3923/ijp.2006.213.215.
Zhang, H., Huang, G., Xu, X., Xiong, Y., Huang, Q., 2018. Estimating evapotranspiration of processing tomato under plastic mulch using the SIMDualKc model. Water 10 (8), 1088. https://doi.org/10.3390/w10081088.
Zhao, N.N., Liu, Y., Cai, J.B., Rosa, R., Paredes, P., Pereira, L.S., 2013. Dual crop coefficient modelling applied to the winter wheat-summer maize crop sequence in North China Plain: basal crop coefficients and soil evaporation component. Agric. Water Manag. 117, 93–105. https://doi.org/10.1016/j.agwat.2012.11.008.